HHS Public Access

Author manuscript

Cell Host Microbe. Author manuscript; available in PMC 2024 February 08.

Published in final edited form as:

Cell Host Microbe. 2023 February 08; 31(2): 213–227.e9. doi:10.1016/j.chom.2022.12.009.

Microbiota-dependent proteolysis of gluten subverts diet-mediated protection against type 1 diabetes

Matthew C. Funsten[1,2,13], **Leonid A. Yurkovetskiy**[2,3,13], **Andrey Kuznetsov**[2], **Derek Reiman**[4], **Camilla H. F. Hansen**[2,5], **Katharine I. Senter**[2], **Jean Lee**[2,6], **Jeremy Ratiu**[7], **Shiva Dahal-Koirala**[8], **Dionysios A. Antonopoulos**[9], **Gary M. Dunny**[10], **Ludvig M. Sollid**[8], **David Serreze**[7], **Aly A. Khan**[1,2,11,12], **Alexander V. Chervonsky**[1,2,3,14,*]

[1]Committee on Immunology, The University of Chicago, Chicago, IL 60637, USA.

[2]Department of Pathology, The University of Chicago, Chicago, IL 60637, USA.

[3]Committee on Microbiology, The University of Chicago, Chicago, IL 60637, USA. Current address: Program in Molecular Medicine, University of Massachusetts Medical School, Worcester, MA 01655, USA.

[4]Toyota Technological Institute at Chicago, Chicago, IL 60637, USA.

[5]Department of Veterinary and Animal Sciences, Faculty of Health and Medical Sciences, University of Copenhagen, DK-1870, Frederiksberg C, Denmark.

[6]Committee on Cancer Biology, The University of Chicago, Chicago, IL 60637, USA.

[7]The Jackson Laboratory, Bar Harbor, ME 04609, USA.

[8]KG Jebsen Coeliac Disease Research Centre and Department of Immunology, University of Oslo and University of Oslo Hospital, 0372 Oslo, Norway.

[9]Biosciences Division, Argonne National Laboratory, Lemont, IL 60439, USA.

[10]Department of Microbiology and Immunology, University of Minnesota, Minneapolis, MN 55455, USA.

[11]Institute for Population and Precision Health, The University of Chicago, Chicago, IL 60637, USA.

[12]Department of Family Medicine, The University of Chicago, Chicago, IL 60637, USA.

[13]These authors contributed equally.

[*]Correspondence: achervon@bsd.uchicago.edu.

Author Contributions

Conceptualization, A.V.C., M.C.F., L.A.Y.; Methodology, M.C.F., A.K., L.A.Y., S.D-K., D.R., A.A.K., G.M.D., D.A.A.; Investigation, M.C.F., L.A.Y., A.K., C.H.F.H., K.S., J.L., J.R., S.D-K., D.R.; Writing- Original Draft, A.V.C., M.C.F.; Writing- Review & Editing, M.C.F., D.S., L.M.S., A.A.K., G.M.D., D.A.A.; Supervision, A.V.C., L.M.S., D.S., A.A.K.; Funding acquisition, A.V.C., L.M.S., D.S.

Declaration of Interests:

We declare no competing interests.

[14]Lead Contact.

Summary

Diet and commensals can affect development of autoimmune diseases like Type 1 diabetes (T1D). However, whether dietary interventions are microbe-mediated was unclear. We found that diet based on hydrolyzed casein (HC) as a protein source protects non-obese diabetic (NOD) mice in conventional and germ-free (GF) conditions via improvement in the physiology of insulin-producing cells to reduce autoimmune activation. Addition of gluten (a cereal protein complex associated with celiac disease) facilitates autoimmunity dependent on microbial proteolysis of gluten: T1D develops in GF animals monocolonized with *Enterococcus faecalis* harboring secreted gluten-digesting proteases, but not in mice colonized with protease deficient bacteria. Gluten digestion by *E. faecalis* generates T cell-activating peptides and promotes innate immunity by enhancing macrophage reactivity to lipopolysaccharide (LPS). Gnotobiotic NOD Toll4-negative mice monocolonized with *E. faecalis* on HC+gluten diet are resistant to T1D. These findings provide insights into strategies to develop dietary interventions to help protect humans against autoimmunity.

Graphical Abstract

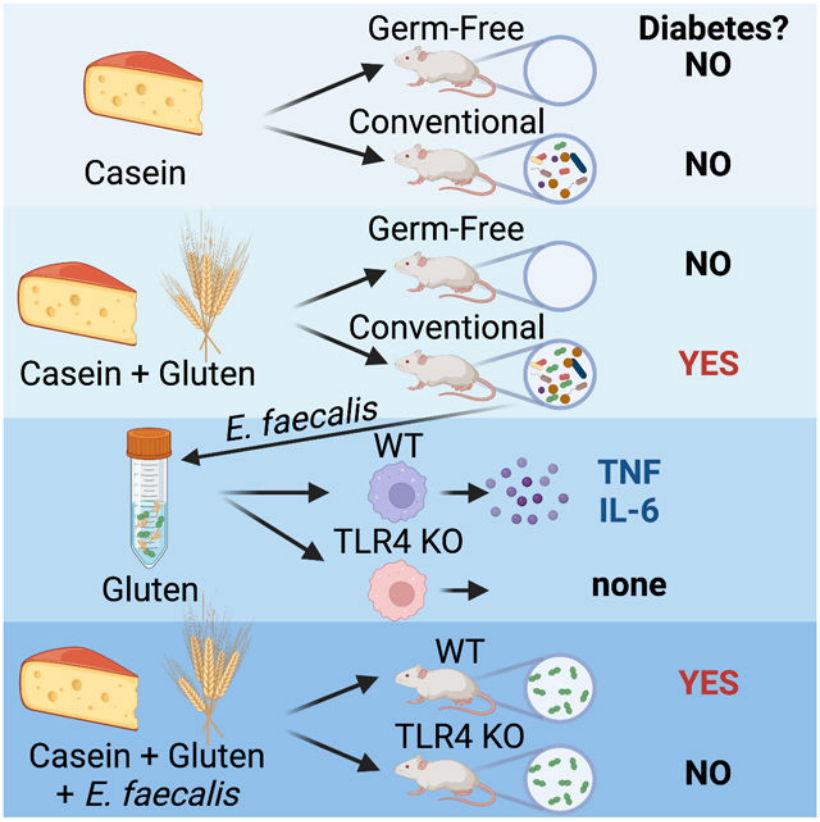

eTOC Blurb

Funsten et al. find that dietary casein attenuates autoimmune diabetes likely by improving the physiology of insulin-producing cells independent of commensals. Gluten and protease-secreting

microbes reverse casein-mediated protection. Gluten proteolysis leads to enhanced activation of innate immunity by gluten-associated microbial products and to enhancement of autoimmune inflammation in the pancreas.

Introduction

Although autoimmunity has a strong genetic basis, environmental factors also contribute to disease development and progression[1]. Diet is one of such factors affecting many physiological and pathophysiological processes. For Type 1 diabetes (T1D), dietary interventions have been reported to affect the disease in animal models and are suspected as modulators of human disease[2-9]. Another environmental factor, the commensal microbiota, plays a role in regulation of the major autoimmune diseases [10-12]. At the same time the microbiota rapidly adapts to dietary changes influencing the physiology of the host[13-17]. Together, these findings predicted that dietary interventions in autoimmunity might be dependent on the microbiota. If that were true, however, the degree of variation in human commensal microbiota composition and function[18,19] would make the prognosis for such interventions rather pessimistic. Thus, identification of dietary interventions that are microbiota-independent as well as dissecting the specific diet-commensal interactions leading to enhancement of organ-specific inflammation/autoimmunity could be of great value.

To study diet-commensal interactions in autoimmunity, we have selected the NOD (non-obese diabetic) mouse model of T1D and applied a diet containing hydrolyzed casein (HC) as the sole amino acid source. This diet has been previously reported to protect both diabetes-prone Non-Obese Diabetic (NOD) mice and Biobreeding (BB) rats including germ-free (GF) rats [6,20-22]. We found that HC also protected NOD mice in the absence of the microbiota in GF mice and that the protection was likely based on the improvement of beta cell physiology. HC protection was reversed by the addition of gluten, but only in the presence of the microbiota. Promotion of islet inflammation by gluten was dependent on microbial ability to digest gluten. Our study provides important mechanistic insights into the microbiota-independent and microbiota-dependent impacts of diet on autoimmunity.

Results

Protection from T1D by HC diet is independent from the microbiota

To test whether the anti-diabetic effect of HC diet was dependent on the microbiota, NOD mice in both Specific-Pathogen Free (SPF) and Germ-Free (GF) conditions were exposed to HC, to the same formulation containing intact casein (IC), or to control diet (chow) (Figures 1A, 1B and S1A, B). Both HC and IC diets were protective in both SPF and GF conditions: the incidence was significantly reduced and in the few mice that became diabetic, the onset of the disease was delayed. Thus, protection from T1D by HC diet depended on the protein source and, very importantly, it was microbiota independent.

To understand the mechanism of protection from T1D, the effects of HC on autoimmune T cells were tested. For that, splenocytes from non-diabetic mice on HC or chow diets

were transferred into immunodeficient NOD.scid (Figure 1C) or NOD.TCRαKO (Figure 1D) recipient mice on chow. There was no difference in development of T1D between the groups. Thus, HC did not induce intrinsic irreparable defects in the autoimmune effector cells. In reverse experiments, T1D development was delayed in NOD.TCRαKO recipient mice on HC diet compared to recipients on regular chow when injected with splenocytes from NOD mice on chow (Figure 1E). Similarly, when naïve $CD4^+$ T cells from BDC2.5 islet-specific T cell receptor (TCR)-transgenic mice[23] were injected into recipient NOD mice fed HC or chow, T cells proliferated stronger in the pancreatic lymph nodes of recipients on chow (Figure 1F). Furthermore, islets of Langerhans isolated from HC fed mice and mixed with splenocytes from TCRαKO mice as a source of antigen presenting cells were less stimulatory to BDC2.5 cells *in vitro* than were islets from chow fed mice (Figure S1C). In addition, we compared the numbers of Tregs in infiltrated islets and the pancreatic lymph nodes (PLN) of mice on chow and HC diets and found no significant differences (Figure S1D). We concluded that HC diet did not affect the ability of mice to generate effector or suppressor T cells, but rather made the target cells, their environment, or both less stimulatory for the autoimmune process.

HC diet affects insulin secretion and beta cell stress

Insulin is a major autoantigen in T1D[24]. To test whether HC affects insulin production/secretion leading to an indirect attenuation of autoimmunity, we used intraperitoneal glucose tolerance test (IPGTT, in which higher insulin secretion results in faster clearance of glucose) in NOD mice fed HC and chow diets. 6-8-week-old female NOD mice on HC diet responded to glucose slower than NOD mice on chow (Figures 2A and 2B, Figures S2A, B) bringing them closer to non-diabetes-prone strains like B6[25]. This observation was also true for TCRα-negative mice (including direct measurements of insulin secretion in response to glucose) (Figures S2C-E), indicating that the slower response to glucose by HC fed mice was independent of the damage inflicted on islets by the adaptive immune system. Importantly, slower clearance of glucose in HC-fed NOD mice could not be explained by an increase in insulin resistance, because they cleared glucose in response to insulin even better than chow-fed NOD mice (Figures 2C and 2D). We also found the fast glucose clearance to be a dominant genetic trait of NOD mice, as (NODxB6)F1 and (B6xNOD)F1 *scid* mice had a reaction to glucose similar to NOD (Figures S2F and S2G)

Enhanced insulin production is associated with beta cell stress[26]. Therefore, isolated islet cells from female NOD.*scid* mice (*scid* mice were used to remove any influence of the adaptive immune system on insulin secretion) fed chow or HC diet were subjected to a single cell RNA sequencing (SCS) analysis. Islets of mice on chow contained a higher proportion of beta cells with high expression of RNA from both mouse insulin encoding genes, *Ins1* and *Ins2* (Figures 2E and 2F). Comparison of gene expression between Ins^{high} and Ins^{low} beta cells (Figure 2G) showed that Ins^{high}, in addition to higher expression of genes involved in insulin secretion itself, also showed upregulated networks of genes involved in unfolded protein response and protein retrotranslocation (Figure 2H), indicative of greater ER stress.

We suggest that the potential mechanism of protection by HC diet is the reduction of intrinsic damage to the islets caused by cellular stress resulting in reduction in the overall damage caused by autoimmunity and the prevention or postponement of hyperglycemia (Figure S2H).

Gluten reverses protection from T1D offered by HC diet

HC diet actively suppresses T1D development. Could other consumed nutrients counteract the benefits of hydrolyzed milk proteins? One alimental component stood out – gluten (a complex of proteins in cereal grains). It was recently shown to impact T1D development in infants[9] and gluten-free diet has been anecdotally reported to reverse T1D in an infant[27]. Thus, we replaced 1/5th of HC with gluten (16%HC +4% gluten of total diet weight, here termed 'HC+4%gluten'). Exposure to HC+4%gluten reversed the protection offered by HC (Figure 2I) when cohorts of mice were exposed to HC, chow and two HC+4%gluten formulations using two different sources of gluten. Direct measurements of insulin secretion by the pancreata of mice on chow, HC, and HC+4%gluten demonstrated that gluten did not increase secretion of the hormone in response to glucose challenge (Figure 2J). In addition, testing glucose tolerance in NOD.scid mice fed HC+4%gluten diet confirmed that gluten did not reverse the reduction of insulin secretion offered by HC (Figures S2I and S2J). At the same time, proliferation of TCR transgenic BDC2.5 cells in the PLN of HC+4%gluten-fed mice was indistinguishable from proliferation in the PLN of mice fed chow (Figure 2K). These results together suggested that gluten does not reverse the positive influence of HC on insulin secretion but rather promotes activation of autoimmunity by other means.

Gluten activates autoimmune process

To test this hypothesis further, we used SCS and multiparameter flow cytometry approaches to compare cell subsets within infiltrated islets. Multiple cell types were affected by the consumption of gluten. Comparison of endocrine cells ratios showed a selective loss of beta cells in 15-week-old NOD mice on HC+4%gluten diet (Figures 3A and 3B and Figure S3A), whereas the remaining beta cells had upregulated TNF (tumor necrosis factor) receptor signaling response genes revealed by gene-set enrichment analysis [GSEA[28,29]] (Figures 3C and S3B). Myeloid cells in the islets also had higher expression of TNF among other genes related to inflammation (Figure 3D). Multi-color immunofluorescence analysis (Figure S3C shows UMAP plot of all detected cell subsets) demonstrated that dendritic cells had higher expression of inducible co-stimulatory molecule CD86 in the HC+4%gluten group (Figure 3E and Figure S3D). T cell subsets were also affected: $FoxP3^-$ T cells in the HC+4%gluten group had higher proliferative activity (staining with anti-Ki67 antibodies, Figure 3F and Figure S3E), whereas FoxP3+ Treg cells in the same group showed stronger expression of the markers of tissue residency[30,31], such as CD103 (Figure 3G and Figure S3G), and others revealed by SCS of islet infiltrates (Figure S3F). That was interpreted as a sign of their activation by a stronger immune response[32].

To further analyze the propensity of gluten to promote autoimmunity, we performed SCS of islet infiltrates from mice fed HC or HC+4%gluten focusing specifically on the state of expansion of T cell clones and the repertoire of their TCRs. It became apparent that islets from mice on HC+4%gluten contained more $CD8^+$ T cell clones with stronger expansion

than mice on HC diet (Figure 3H and Figure S4A). Analysis of the complementarity determining region 3 (CDR3) segments of the TCR alpha chains (Figure 3I) revealed an expansion of sequences identical or visibly close to CDR3α of highly diabetogenic NY8.3 TCR specific to islet-specific glucose-6-phosphate related subunit (IGRP)[33,34]) in mice fed HC+4%gluten diet. Moreover, sequence similarity analysis using BLOSUm62 scoring matrix revealed additional CDR3α sequences with high probability of conferring the same specificity (Figure 3J). Beta chains were also more clonally expanded in mice consuming gluten (Figure S4A), but they were clearly more diverse than alpha chains (Figure S4B), a phenomenon noted before[35]. Supporting our findings were functional data (IFN-γ secretion) showing an expansion of IGRP-reactive $CD8^+$ T cells in the regional lymph nodes of HC+4%gluten fed mice compared to HC-fed mice (Figure 3K). That was also true for other epitopes recognized by diabetogenic T cells (Figure S4C). Interestingly, the clonal expansion was more obvious among $CD8^+$ T cells compared to $CD4^+$ cells in the same infiltrate (Figure S4D-G). In sum, gluten clearly enhanced immune activation resulting in damage to insulin-producing cells overcoming the positive effect of HC diet.

Enhancement of autoimmunity by gluten requires the microbiota

To test whether gluten's contribution to T1D was microbiota-dependent, we repeated exposure to HC+4%gluten diet in germ-free conditions. GF NOD mice on HC+4%gluten did not develop T1D (Figure 4A).

Such dependence on the microbiota required a plausible explanation. One possibility related to the role of gluten in celiac disease, was microbial activation of transglutaminase 2 (TGM2), an enzyme that can post-translationally modify glutamines in antigenic peptides by deamidation or transamidation (cross-linking)[36]. To test whether TGM2 activation was involved in T1D promotion by gluten, we used CRISPR/CAS9 to target the *Tgm2* gene in NOD mice (Figure S5A). Despite the lack of TGM2 protein (Figure S5B), T1D development was not affected in NOD.TGM2 KO mice fed regular chow or even HC+4%gluten diet (Figure 4B). Mutants were also tested at another institution (The Jackson Laboratory) to minimize a potential influence of different microbiomes (Figure S5C).

Thus, a different mechanism such as microbial catabolism of gluten producing biologically active fragments, must be responsible for gluten's microbe-dependent pro-diabetic activity. First, we tested whether availability of gluten as a nutrition source for the microbiota affected the structure of the microbial communities in the small intestine (SI) and cecum of mice. Groups of GF NOD mice were colonized with the same microbiota taken from SPF NOD mice [it was important to standardize the input microbiota in order to avoid legacy effects[37]] (Figure S5D). 16S rRNA bacterial genes analysis revealed that the SI microbes from HC-fed mice were quite different from microbes from chow- and gluten-fed mice, whereas the latter two groups were rather similar (Figure 4C). Interestingly, that was not true for cecal microbiotas: there the microbial communities in mice on HC and HC+4%gluten diets were similar to each other, and both separated clearly from bacteria from mice on chow (Figure 4E). The abundances of the top lineages in all groups are shown in Figures 4D and 4F. Thus, one should expect bacteria utilizing gluten to be present primarily in the SI where gluten is being digested by microbial and host enzymes. To identify gluten-

digesting bacteria in the SI of HC+4%gluten fed NOD mice, SI bacteria were plated on agar supplemented with an ethanol extract of gliadin, a component of gluten. The opaque agar plates allowed detection of colonies that secreted proteases cleaving gliadin and leaving transparent halos around positive colonies (Figure 4G). Isolated colonies were identified by 16S rRNA genes sequencing. Most of these colonies were classified as *Enterococcus faecalis* (*E. faecalis*).

Using *E. faecalis*. a Gram-positive bacterium with tractable genetics, allowed us to test the hypothesis that processing of gluten by the microbiota yields biologically active molecules that contribute to innate and/or adaptive immune activation creating an inflammatory environment.

Gluten proteolysis by bacteria leads to activation of adaptive immunity

Gluten proteins are barely soluble in buffers with physiological salt concentrations[38]. We reasoned that proteolysis could liberate peptides that would stimulate either adaptive or innate arms of immunity. Bacterial digests of gluten were added to a mixture of mouse lymphoma cell line 578_BV7_AV12 (.578) carrying a human T cell receptor against a gliadin-ω2-derived peptide[39] and human transformed B cell lines carrying HLA-DQ2.5 MHC class II molecules. Addition of bacterial digest of gluten to T cells and antigen-presenting cells induced IL-2 secretion by responder T cells (Figure 5A). That was true for additional randomly picked *E. faecalis* colonies from different SPF NOD mice (Figure S6A). The effect of T cell activation was specific, as a different T cell specific for gliadin alpha1 peptide/HLA-DQ8 complex, TCC489.2.14 (.489)[40], did not react to the digest but was reactive to its own cognate peptide (Figure 5A). The presence of peptide recognized by .578 T cells was already detectable after three hours of digestion and peaked at around six hours (Figure S6B). Mutant bacteria with site-directed mutagenesis inactivation of *fsrB* operon regulating two secreted proteases GelE and SprE failed to digest gliadin (Figure 5B) and to stimulate IL-2 production by gliadin-specific T cells (which was also true for cell-free bacterial culture supernatant used as a source of proteases) (Figure 5C). Antigenic peptide-liberating activity was entirely dependent on GelE protease: *E. faecalis* strain TX5264[41] lacking *gelE* due to site-directed mutagenesis was incapable of producing the activating peptide, whereas the same strain reconstituted with *gelE* under heterologous promoter had that property restored (Figure 5D). Thus, proteases secreted by pro-diabetic bacteria can liberate immunogenic peptides cognate for the adaptive immune system.

Gluten proteolysis leads to activation of innate immunity

To test the role of gluten proteolysis in innate immune system activation, we exposed peritoneal macrophages to bacterial gluten digests and tested culture supernatants for a short-term response (6 hrs, TNF secretion) and for a delayed response [overnight, interleukin 6 (IL-6) secretion]. Bacterial medium alone was predictably stimulatory in this assay, thus we replaced it with tissue culture medium DMEM to grow *E. faecalis* in the presence of gluten. Filtered supernatant was capable of eliciting secretion of both cytokines (Figures 5E and 5F) from peritoneal as well as pancreatic lymph node macrophages (Figures S6C and S6D). Induction of cytokines was dependent on bacterial proteases (Figures 5E and 5F) and, importantly, it was specific for gluten, as other proteins digested by *E. faecalis* were not as

stimulatory (Figure S6E). It was also mostly due to SprE protease as *sprE* negative bacteria TX5243[42] showed significantly reduced induction of TNF upon digestion of gluten (Figure 5G), whereas a *gelE*-negative mutant had even stronger TNF-inducing capacity. That was consistent with the data on negative proteolytic regulation of SprE by GelE protease[43].

Cytokine secretion triggered by proteolytic digest of gluten depends on lipopolysaccharide (LPS)

Although clearly dependent on the proteolysis, cytokine secretion was surprisingly resistant to heat treatment of the gluten digest or an additional treatment with mammalian protease trypsin (Figures 6A and 6B). Notably, gluten incubated in DMEM at 37°C overnight by itself elicited low level cytokine secretion that was also insensitive to heat and trypsin. Although gluten can be hydrolyzed to a limited extent in salt-containing solutions, heat resistance of cytokine induction suggested that gluten may contain a non-proteinaceous stimulatory moiety. Thus, we treated the digests with bead-bound Polymyxin B, an LPS-inactivating antibiotic compound. That treatment prevented macrophage activation by both bacterial digests of gluten and by gluten incubated in DMEM (Figure 6C). Moreover, macrophages lacking the MyD88 adaptor or Toll-like receptor 4 (TLR4) LPS receptor were not activated by gluten digests (Figure 6D) and LPS could be detected in gluten and commercial flour products by a Limulus amebocyte lysate (LAL) assay (Figure S7A). Thus, it appeared that microbial digestion of gluten liberated LPS (or another hydrophobic lipid moiety that behaves like LPS) naturally associated with gluten.

Stronger stimulation of the innate response by gluten digest compared to gluten alone was not simply an additive effect of LPS (i.e. more LPS was liberated upon more efficient gluten digestion). That became clear when suboptimal concentrations of LPS (Figure S7B) were used to elicit cytokine secretion from macrophages in the presence of the bacterial digest of gluten (Figure 6E). In both cases, cytokine secretion was enhanced beyond the simple sum of responses triggered by TLR agonists and by bacterial digest of gluten. Importantly, the enhancement of suboptimal LPS could be only seen if hexa-acylated LPS from *Proteobacteria* but not penta-acylated LPS from *Bacteroides* was used (Figure S7C and S7D).

Importantly, several other SI bacteria were identified as gluten consumers (growing on minimal medium supplemented with gluten) and the digests of gluten by these bacteria were tested for their ability to elicit inflammatory cytokines. When gluten digests were performed keeping bacteria at exponential growth, at least two other bacterial lineages were found capable of inducing strong TNF secretion in wild-type macrophages and did not elicit a response from TLR4-negative macrophages (Figure 6F).

Gluten digestion by secreted microbial proteases is key to T1D promotion

To test whether monocolonization of GF mice with *E. faecalis* would promote T1D development, we set up an observation experiment. Gnotobiotic mice monocolonized with human isolate of *E. faecalis* OG1RF[44] were fed HC+4%gluten diet. A clone (TX5266)[45] of the same strain with a directly mutagenized *fsrB* operon controlling these proteases was used as a negative control. NOD mice monocolonized with the wild-type *E. faecalis* strain and

fed HC+4% gluten diet showed markedly increased incidence of T1D development (Figure 7A) compared to GF mice fed the same diet, whereas those colonized with the mutant strain did not. The incidence of T1D was somewhat lower than we normally observe in GF mice on regular diet, but subsequent analysis revealed that in mice that stayed T1D-free, the wild-type *E. faecalis* bacteria had lost the ability to digest gluten *via* secreted proteases (Figure 7B). These results strongly suggested that the proteolytic cleavage of gluten by bacterial enzymes was in fact the key to advancement of autoimmunity. Finally, to test the role of LPS-driven signaling in T1D development *in vivo*, we took advantage of the GF TLR4 KO NOD mice, which develop T1D normally when fed chow diet [46]. Mice were put on HC+4%gluten diet and monocolonized with *E. faecalis*. The T1D incidence in this group was significantly lower compared to the wild-type controls (Figure 7C).

Discussion

For testing the role of diet in protection from T1D, the choice of hydrolyzed casein was not random: many independent reports confirmed its protective properties in T1D development in SPF mice, already suggesting that given the microbiota variability between experimental sites, the protection may have been microbiota independent. The use of this diet in GF NOD mice that are highly sensitive to T1D[10] has confirmed that idea also indicating that casein has an active role in protection from T1D since mice on chow diet rich in gluten were not protected in both SPF and GF conditions. We have found that the protection was not associated with the active suppression of the immune effector mechanisms, but rather due to reduction of the initial sensitization steps. We and others[47,48] have predicted that the intrinsic health status of the target organ could affect the initiation of autoimmunity. A more recent theoretical model linked hormone hypersecretion with autoimmunity[49]. It suggested that endocrine cells that acquire positive signal from metabolites that they regulate (e.g. glucose) may tend to expand and undergo malignant transformation. The immune response is expected to remove such cells. Our data provided experimental support for these ideas: reduced levels of insulin secretion by the islets of Langerhans also reduced their destruction by autoimmunity. This reduction of insulin secretion by HC diet was independent of the damage from the adaptive immune system suggesting a direct influence on hormone-secreting cells. Fasting serum insulin levels were moderately lower in HC-fed mice compared to the chow controls (Figure 2J), which could also be due to lesser insulin resistance in HC-fed mice. SCS confirmed that pancreatic islets of mice fed regular chow contained more beta cells with higher insulin expression and signs of associated cell stress. However, the increased expression of both mouse insulin genes may not be the only mechanism leading to higher glucose tolerance in mice on chow, as hormone secretion has a complex regulation *in vivo* and may affect the amount of available systemic insulin post-transcriptionally. How exactly casein regulates insulin secretion still needs to be elucidated. Regardless, the ability to activate autoimmunity was reduced in HC-fed animals. Since insulin is considered to be the most significant antigen in T1D development [24], we propose a model explaining how reduction in insulin secretion reduces autoimmunity and improves the physiology of beta cells (Figure S2H). Our model is supported by reduced activation of islet-specific T cells both *in vivo* and *in vitro* (Figures 1F and S1C). We have previously reported that the severe reduction of insulin secretion caused by *Akita* mutation even made

mice and beta cells more resistant to insulin-specific T cells [50]. That is unlikely to be the case for HC diet, where insulin secretion is moderately reduced leaving beta cells sensitive enough for killing.

It needs to be noted that other polypeptides known to be autoantigens (e.g. Chromogranin A, IA-2 transmembrane phosphatase and Zn transporter 8) [51-53] are also components of the secretory granules. Thus, autoimmune responses to them should also be stimulated by increased insulin secretion. This is an indirect model of reduced autoimmune activation due to reduction of the antigen supply. However, the reduction of activation of autoimmunity could be also due to more direct effects of hydrolyzed casein on APCs. Such mechanism has been suggested in the BB rat model of HC protection[22]. On the other hand, proposed direct effect of HC diet on beta cells better explains its independence from the microbiota: it bypasses the immune system, which is highly sensitive to modifications by the microbiota.

In our experiments, HC was introduced at the pregnancy stage and the progeny were always kept on that diet. In human infants prone to T1D, however, when HC formula was introduced after birth, the treatment was not as successful [54]. Both the timing of diet introduction and the influence of consumption of other dietary products supplementing the formula could have played a role. Gluten was a natural choice for subsequent experiments because of recent studies supporting the role of gluten in diabetogenesis in humans[9] and because gluten drives the pathogenesis of celiac disease, which is also observed in a significant fraction of T1D patients[55,56]. In fact, gluten reversed the protection offered by HC and did it in a microbiota-dependent manner. GF mice consuming HC+4%gluten diet, were still protected. Since gluten did not affect glucose tolerance compared to HC diet (Figures 2A and S2I, J), we suggested that gluten enhanced autoimmunity by acting on the immune system directly. This idea was confirmed by functional transfer tests, by single-cell RNA sequencing and by multicolor immunofluorescence analysis. TCRs with specificity to IGRP conferred by alpha chains [lesser importance of beta chains was previously demonstrated[35,57]] and their enhanced activation in the pancreatic lymph nodes (Figure 3I-K) demonstrated that gluten promoted known diabetogenic mechanisms.

Microbial interactions with gluten leading to T1D enhancement were independent of TGM2 but were dependent on the ability of microbial proteases to digest gluten. One of the gluten-digesting bacteria, *E. faecalis* was able to trigger diabetes development in gnotobiotic NOD mice receiving HC+4%gluten diet, provided that they expressed two secreted proteases GelE and SprE. These two proteases conferred different functions: GelE was required for the ability of *E. faecalis* to liberate peptides recognized by T cells carrying receptors isolated from celiac disease patients. SprE was not capable of doing that, but instead was much more efficient at releasing LPS from gluten to stimulate innate immune cells to produce pro-inflammatory cytokines. LPS is a product of gram-negative bacteria and is not produced by gram-positive *E. faecalis*. We found, however, different levels of LPS contamination in commercial gluten and flour products. The enhancement of pro-inflammatory effect of LPS was synergistic between LPS and the products of digestion, the latter possibly affecting LPS aggregation and the binding of LPS monomers to the CD14 co-receptor on the surface of macrophages. Such enhancement is not unprecedented: LPS bound by a retrovirus[58] or by heat-shock proteins[59,60] is far more potent than LPS directly added to innate cells.

Sensitivities to heat and to Polymyxin B set the observed macrophage activation apart from TLR4-mediated response induced by wheat amylase trypsin inhibitors also found in glutens[61]. Previously, microbial PAMPs (including LPS) were shown to reduce T1D in NOD mice[11,62]. However, in these experiments, LPS was delivered systemically potentially inducing protective mechanisms that cannot be stimulated from inside the gut[63]. LPS is already plentiful in the normal gut inducing LPS tolerance in local myeloid cells, so why would gluten-associated LPS make a difference? As we have shown, the enhancement of macrophage response to LPS only happens with hexa-acylated LPS and not penta-acylated variety (Figure S7C and S7D). Since penta-acylated LPS dominates in mammalian gut[11], it is possible that gluten-associated LPS is hexa-acylated. Another possibility to explain the diabetogenic tole of gluten-associated LPS is that association with the products of gluten digestion allows efficient delivery of LPS to the pancreatic lymph nodes, where it can activate local myeloid cells and promote T1D. In fact, we found that macrophages in the pancreatic and SI draining lymph nodes were not tolerant of LPS and were excitable to produce TNF in response to gluten digested with *E. faecalis* (Figures S6C and S6D). Although this intriguing mechanism(s) is yet to be elucidated, the requirement for TLR4 in GF mice to develop T1D when monocolonized with *E. faecalis* and fed HC+4%gluten diet (Figure 7C) clearly demonstrated that gluten-LPS combination was diabetogenic. These experiments suggest that LPS presentation could be a major mechanism of T1D promotion by gluten. However, we cannot fully disregard the ability of gluten digestion to induce adaptive T cell responses. Whether such T cells are cross-reactive with islet antigens or simply provide an inflammatory mileu in the gut- and pancreas-draining lymph nodes (bystander activation) remains to be elucidated.

Our experiments were focused on *E. faecalis* because of its dominance in the gliadin digestion assay. Other bacteria either producing halos on gliadin plates or capable of growing on gluten-containing minimal medium plates were tested for elicitation of TNF secretion by macrophages (Figure 6F). When grown on DMEM/gluten, other bacteria stimulated production of TNF by macrophages. Thus, bacteria other than *E. faecalis* could induce similar phenotypes, likely due to their own secreted proteases. It has also been suggested that other bacterial proteases (e.g. elastase from *Pseudomonas aeruginosa*) can promote inflammatory responses by digesting gluten[64] making *E. faecalis* not a protagonist, but rather a prototype for a particular biological activity (gluten proteolysis) that can lead to disease development. This conclusion is important, because in various mouse colonies and in the vast human population individual microbiomes may have genes expressed by different bacteria that would encode proteases with similar functions. Restoration of T1D by *E. faecalis* in gnotobiotic mice on HC+4%gluten diet compared to GF mice on the same diet (Figure 7) was not to its full extent leaving a role (quantitative or qualitative) for other members of microbial communities to promote disease after gluten consumption.

In sum, our results make two major points. First, as we have previously suggested [47], changing the physiology of the target organ (such as insulin secretion) may abrogate or delay the pathological process of the activation of autoimmunity. That can be achieved by relatively simple low-cost approaches that could be applied regardless of the complexity of the individual's microbiota. And second, dietary components (such as gluten) require processing by the members of microbial communities to provoke development

of autoimmunity. Two important biological activities of intestinal microbes linked to the proteolytic digestion of gluten – production of peptides activating adaptive immunity and increasing the potency of LPS-mediated stimulation of the innate immunity – were identified.

Recent analysis of infants predisposed to T1D has pointed at gluten as a pathogenicity factor[9]. Whether other proteins can utilize similar mechanisms (overcoming positive effects of milk proteins or on their own) is very important along with elucidation of underlying mechanisms for development of prophylactic interventions in autoimmunity. We expect our findings to lead to new approaches to protection from autoimmunity and inflammation.

Limitations of the Study

The molecular mechanism of hydrolyzed casein's effects on insulin secretion or on the activation of APC have not been fully elucidated yet. Similarly, the precise mechanism of enhancement of LPS activity by microbially digested gluten and its contribution to T1D pathogenesis relative to contribution of liberated T cell activating gluten peptides warrants further investigation.

STAR Methods

Resource Availability

Lead Contact—Further information and requests for resources and reagents should be directed to and will be fulfilled by the lead contact, Alexander Chervonsky (achervon@bsd.uchicago.edu).

Materials Availability

NOD.TGM2 KO mice generated in this study will be available from AVC lab for 6 months after publication and after that from The Jackson Laboratory frozen stock (Stock#29497 is NOD/ShiLtDvs-Tgm2<em1Dvs>/Dvs).

Data and Code Availability

Single-cell RNA-seq and TCR sequencing data have been deposited at GEO and are publicly available as of the date of publication. Accession numbers are listed in the key resources table. 16s rRNA sequencing data have been deposited to GitHub and are publicly available as of the date of publication. The web-address to access the 16S data is listed in the key resources table. This paper does not report original code. Any additional information required to reanalyze the data reported in this paper is available from the lead contact upon request.

Experimental Model and Subject Details

Animals—NOD/ShiLtJ (RRID:IMSR_JAX:001976), NOD.Cg-*Prkdc*^{scid}/J (NOD.SCID, RRID:IMSR_JAX:001303), NOD.129P2(C)-*Tcra*^{tm1Mjo}/DoiJ (NOD.TCRa KO, RRID:IMSR_JAX:004444), and NOD.Cg-Tg(TcraBDC2.5,TcrbBDC2.5)1Doi/DoiJ (NOD.BDC2.5, RRID:IMSR_JAX:004460) mice were purchased from The Jackson Laboratory (Bar Harbor, ME;) and bred in house. B6.MyD88 KO mice were a gift

from S. Akira and backcrossed to NOD/ShiLtJ mice for more than 10 generations as previously described (NOD.MyD88 KO, Wen, *et al.* 2008) and are currently bred in house. C57BL/10ScN mice were originally purchased from NIH (now at Jackson Labs, RRID:IMSR_JAX:003752) and backcrossed to NOD/ShiLtJ for more than 10 generations as previously described (NOD.TLR4 KO, Burrows, *et al. PNAS.* 2015) and are currently bred in house. NOD.TGM2 KO mice were produced using CRISPR/Cas9 technology. *Tgm2* exons 1 and 2 were targeted by the guides 5'-GTCGCCGCTAGCCTGG-3' and 5'-GATTTGGAGATTCAGGC-3' respectively to produce a dropout mutation between the two cut sites. Lack of TGM2 protein expression in the knockout mice was confirmed by western blotting (Fig. S5B, see methods below). All animals were kept under SPF conditions and NOD/ShiLtJ, NOD.MyD88 KO and NOD.TLR4 KO were kept under GF conditions at the University of Chicago Animal Resource Center. GF status was monitored by aerobic and anaerobic fecal cultures and PCR amplification of bacterial 16S rRNA genes from fecal DNA as previously described [66].

Gnotobiotic NOD mice were derived at 4 weeks of age from GF mice by introduction of bacteria via gastric gavage of cecal content taken from an SPF NOD/ShiLtJ mouse. Mice were placed on different diets and their cecal and small intestine contents were isolated after 8 weeks for 16S rRNA gene analysis. For colonization with *E. faecalis*, mating pairs were placed on Casein+4%gluten diet and gavaged with wild-type or mutant bacteria. Bacteria were transferred to the progeny naturally from the mother, and the accuracy of colonization of the progeny was confirmed by PCR targeting the 16S rRNA encoding gene (using fecal DNA) followed by sequencing. Colonization levels for wild-type and mutant *E. faecalis* were similar: $(35\pm10)x10^5$ and $(45\pm14)x10^5$ colonies per 100μl of the cecal contents, respectively.

Purified diets were prepared by Envigo (Madison, WI) utilizing hydrolyzed (TD. 120338) and intact (TD. 120337) caseins from AMCO (Burlington, NJ). Gluten-containing diets (TD. 150366 and TD. 130340) were based on TD. 120338 and contained 4% of gluten protein from wheat gluten supplied by ADM (WhetPro 80) (Gluten 1) or by Mallindra Milling corporation (Gem of the West) (Gluten 2), respectively. Diets were vacuum packaged and irradiated (20-50 kGy range) and tested for a microbial panel before being given to mice in germ-free and SPF housing. Standard chow diet in our facilities was NIH-31 modified open formula 7013 from Envigo. This diet contains 35.5% wheat (contains about 10% protein) and 10% wheat middlings (contain about 16% protein). Total wheat protein is about 5.2% in the chow diet. Assuming gluten constituting between 70% and 75% of wheat protein[67], its contents in chow diet is around 4%. That is similar to HC+4%gluten diet TD. 130340 diet. In all T1D-related experiments, the respective diets were administered to mothers throughout pregnancy and until pups were weaned and kept on the same diets until 30 weeks of age. In microbiota testing experiment, diets were introduced to GF mice simultaneously with colonization with SPF microbiota at weaning.

Unless noted otherwise, female mice were used in all experiments. All experiments were performed in accordance with both The University of Chicago Animal Care and Use Committee and national guidelines.

Microbial Strains—OG1RF – parental strain[44], (*gelE+, sprE+*); TX5266 – OG1RF Δ*fsrB*, (*gelE−, sprE−*)[45] (direct mutagenesis), TX5243[41] (*gelE+, sprE−*) (direct mutagenesis), a generous gift from Dr. Barbara Murray (UT Health Science Center, Houston), TX5264[42] (*gelE−, sprE+*) (direct mutagenesis) (JRC105 – OG1RF Δ(*gelE−sprE*) (direct mutagenesis)[68] were grown anaerobically or aerobically in Bacto Brain Heart Infusion (BHI) (Becton, Dickenson & Company, Sparks, MD) broth at 37°C with shaking for 16 – 18 hrs.

TX5264 mutant bacteria transformed with either empty shuttle vector containing nisin-inducible promoter pMSP3535[69], or *gelE* gene in the same plasmid[70] were used to test the role of GelE in liberation of antigenic peptides from gluten. The cultures were supplemented with 10μg/ml Erythromycin +/− (Sigma) and 25ng/ml nisin (Sigma).

Method Details

Diabetes Testing—Diabetes development was monitored by weekly testing of urine glucose with Diastix strips (Bayer, Elkhart, IN). Islet infiltration was scored in a blinded fashion and graded as follows: 0, no visible infiltration; I, periinsulitis; II, insulitis with <50%; and III, insulitis with >50% islet infiltration. 20+ 5-μm sections spaced 40-μm apart were collected and scored for each pancreas. At least 100 islets in each group of 14 mice were scored.

Splenocyte transfer—Single cell suspensions were prepared from non-diabetic 10–13-week-old NOD female mice on either HC or regular chow diet. Red blood cells were lysed by suspension of cell pellets in 900μl sterile, distilled water (Gibco) for 10 seconds followed by addition of 100μl 10X PBS. Cells were then spun down and resuspended in PBS. $2x10^7$ cells were injected intravenously into recipient mice. Recipient mice were monitored for diabetes development weekly by measuring urine glucose with Diastix (Bayer, Elkhart, IN).

T cell proliferation *in vivo*—CD4 T cells were enriched using anti-CD4 magnetic beads (Miltenyi Biotec, Auburn, CA) from splenocytes of NOD mice carrying the transgene for BDC2.5 TCR. T cells were labeled with 5uM carboxyfluorescein succinimidyl ester (CFSE) (Molecular Probes, Eugene, OR) for 15 minutes at 20°C followed by two washes in Click's Medium (Irvine Scientific, Santa Ana, CA) containing 5% FCS (Atlanta Biologicals, Lawrenceville, GA) followed by resuspension in PBS. $1.5\text{-}2x10^6$ T cells were transferred intravenously to recipient mice on different diets. Pancreatic and non-draining lymph nodes were harvested 72 hours post transfer and analyzed for CFSE dilution by FACS on an LSR-II flow cytometer and analyzed using FlowJo software (Treestar).

***In vitro* proliferation of T cells—**$5x10^4$ T-cells were mixed with $5x10^5$ NOD.TCRαKO splenocytes serving as antigen-presenting cells, in Click's Media with 5%FCS. Increasing numbers of islet cells, prepared by digestion with Trypsin-EDTA, were used as a source of antigen. CFSE dilution was analyzed using a LSRII flow cytometer (BD Biosciences, San Jose, CA).

ELISPOT Analysis—2×10^5 PLN cells from NOD females fed either HC or HC+4% gluten and 4×10^5 NOD splenocytes, depleted of CD3ε+ cells (Miltenyi Biotec, Auburn,

CA) according to the manufacturer's instructions, were incubated overnight with 1μg/ml NRPA7 mimic peptide recognized by 8.3 TCRs[71], 1μg/ml mimic peptide recognized by AI4 TCRs[72] or 10μg/ml InsB 15-23 peptide recognized by G9C8 TCRs[73] in 96-well Immobilon-P membrane plate (Millipore) pre-treated with anti-IFN-γ antibodies (BD Bioscience). Plates were treated and spots revealed according to the manufacturer's instructions. Background spots produced (no peptide control) were subtracted from the total spot count in wells with peptide. Results are an average of three parallels. PLN cells from each mouse were also stained with α-CD3ε, -TCRβ, -CD4, and -CD8α antibodies (Biolegend) to calculate the frequency of peptide-specific cells per 10^6 CD8+ αβ-T cells.

Intraperitoneal Glucose Tolerance Test (IPGTT) and Intraperitoneal Insulin Tolerance Test (IPITT)—IPGTT was performed as follows: mice were fasted for 12 h and tested for baseline of blood glucose levels prior to glucose administration. Mice were then injected i.p. with a 20% glucose solution in PBS (2 g/kg body weight) and blood glucose levels measured by glucometer before and 15, 30, 60, 90 and 120 minutes after injection. Data are presented as the difference in glucose levels between each timepoint and time 0.

IPITT was performed by fasting mice for 4h prior to the test. Baseline glucose measurement was made before i.p. injection of 1U/kg insulin (Sigma) followed by measurement of glucose at 15-, 30-, and 60-min. Data are expressed as percent of starting glucose levels.

Measurement of serum insulin levels following glucose challenge—Mice were fasted for 8 hours. After fasting, cheek blood was collected into sterile collection tubes either immediately (fasting insulin) or 5 minutes after an i.p. injection with sterile 20% glucose solution in PBS (2 g/kg body weight). Serum was spun down at 8,000 g. for 8 minutes at 4°C to remove remaining cellular debris. Insulin concentration was measured using the Mouse Insulin ELISA Kit (Alpco) according to the manufacturer's instructions.

Isolation of murine Pancreatic Islets of Langerhans—Mice were killed by cervical dislocation and the pancreata were perfused with 5 mL of collagenase P solution [0.5 mg/ml, (Roche) in HBSS (Gibco) supplemented with 0.1 M HEPES, 1 mM $MgCl_2$, 5 mM D-glucose, 1.25 mM $MgCl_2$, and 0.02% BSA] via the common bile duct. Perfused pancreata were then dissected away from the surrounding tissue and incubated for 10 minutes at 37°C. Digestion was halted by washing the tissue twice with supplemented HBSS. The tissue was then applied to a Histopaque-1119 (Sigma) gradient, and the interface was collected, washed in supplemented HBSS, and then placed in Click's medium with 5% FBS. Islets were handpicked using an inverted microscope. For single-cell RNA sequencing experiments, handpicked islets were dissociated by incubation in Trypsin-EDTA (Gibco) at 37° C for 2 minutes followed by washing in Click's media containing 10% FBS. For flow cytometry of islet infiltrates, handpicked islets were dissociated by incubation in enzyme free cell dissociation buffer (Gibco) for 3 minutes at 37° C followed by washing in Click's media containing 5% FBS.

Single Cell RNA Sequencing—Cells were loaded onto a Chromium Controller (10X Genomics)[74] and processed using the Chromium Single Cell 3' Library & Gel Bead

Kit (10x Genomix, v3) according to the manufacturer's protocol. cDNA and library quality were assessed using the Agilent 2100 Bioanalyzer (Agilent Technologies, Palo Alto, CA). Samples were sequenced using the Ilumina HiSeq 4000 (Ilumina, San Diego, CA). All single cell barcoding, library preparation, quality assessment, and sequencing were performed at the Functional Genomics Facility at the University of Chicago. For experiments using NOD wild-type mice, sequencing was done on one pool per biological condition with three 15-week-old mice in each pool. For experiments using NOD.scid mice, three individual 8-10-week-old mice per biological condition were sequenced. One HC fed NOD.scid sample was removed from the analysis due to very low numbers of reads per cell. Raw sequencing files were processed through the CellRanger pipeline (version 4.0.0) to conduct all alignment and gene expression quantification steps using the mm10 reference mouse genome.

Single-cell data processing—Single cell gene expression data were input into the Seurat Package (version 3.1.5)[75] using R (version 3.6.3). Doublets and dead cells were removed from further analysis by filtering out cells with detectable gene expression in less than 200 genes or greater than 7500, and mitochondrial gene content represented greater than 25% of all genes expressed. Gene expression count matrices were normalized using a global-scale normalization function LogNormalize. Variable features for downstream analysis were identified using the FindVariableFeatures function using the default of 2000 variable features. Cell clustering was performed by first transforming the data with the ScaleData function, performing linear dimensional reduction using RunPCA, and then FindClusters and RunUMAP were used to finish the cell clustering and project the visualization into a two-dimensional space. Cell types were annotated using variable genes that drove separation between different clusters (*Ins1*- β-cells; *Gcg* - α-cells; *Sst*- *δ*-cells; *Cd3d*- T cells; *Ms4a1* - B cells; *Adgre1* - Macrophages; Cd209a - pDC's; *Cdh5*- Endothelial cells; *Col1a1*- stromal cells; also see Fig. S2A). Due to low cell numbers, DC's and macrophages were grouped together as myeloid cells for subsequent analysis. Seurat clusters defined by canonical markers from multiple cell types (*Cd3e* and *Cd79a* for example) were deemed aggregates of multiple cells and removed from the analysis. For comparison of *Ins1* High and *Ins1* Low β-cells in chow fed NOD.SCID mice, *Ins1* High and Low β-cells were defined as β-cells with *Ins1* levels of above 9.0 or below 8.5 log total sum scaled counts respectively. Kernel density estimation was used to define the probability density function of beta cells based on *Ins1* and *Ins2* expression levels within each diet.

Differential gene expression analysis was preformed using the scanpy Python package (version 1.4.5.1)[76]. Batch effects were removed using scanpy's implementation of ComBat, using the sample sequencing run dates as the batch keys. Differential expression was tested for using the rank_gene_groups function with the "t-test_overestim_var" method. P-values were adjusted using the Benjamini-Hochberg method and significant genes were selected as those with a log fold change magnitude greater than 0.5 and an adjusted p-value less than 0.05.

For further analysis of $Ins1^{High}$ vs $Ins1^{Low}$ beta cells, genes upregulated in $Ins1^{High}$ beta cells (log2 fold change > 0.4, adjusted p-value < 0.05) were input into the STRING database[65], which analyzes known and predicted gene-gene interactions. Genes with no

connections were removed from the analysis. From this analysis, 3 clusters were identified that contained genes involved in 1) Insulin processing and secretion; 2) Unfolded protein response and endoplasmic reticulum (ER) associated protein degradation; and 3) Protein processing in the ER. GSEA analysis was carried out using GSEA software v4.1.0[28,29] using the publicly available Hallmark gene sets (h.all.v7.4.symbols.gmt).

TCR Sequencing—Single cell suspensions of islets from 3 HC fed and 3 HC+4%gluten fed 16-week-old NOD mice were washed in 1X PBS supplemented with 1% FBS and 0.05% NaN_3. To block Fc receptors, cells were treated with anti-mouse CD16/32 antibodies (Biolegend, 101301) for 10 minutes at 4° C. Individual samples were then incubated with 2.5 μg/ml of unique Total-Seq™-C antibodies (Biolegend; see Key Resources Table) for 30 minutes at 4° C and then washed again with 1X PBS supplemented with 1% FBS and 0.05% NaN_3. Cells were then pooled, split into four batches, and each batch was loaded onto a Chromium Controller (10X Genomics)[74] and processed using the Chromium Single Cell 5' Library & Gel Bead Kit, Chromium single cell mouse TCR amplification kit, and the Chromium single cell 5' library construction kit (10x Genomix) according to the manufacturer's protocol. cDNA and library quality were assessed using the Agilent 2100 Bioanalyzer (Agilent Technologies, Palo Alto, CA). Samples were sequenced in two runs using the Ilumina NovaSeq 6000 (Ilumina, San Diego, CA). All single cell barcoding, library preparation, quality assessment, and sequencing were performed at the Functional Genomics Facility at the University of Chicago.

Filtered_contig_annotation.csv and clonotypes.csv files were generated using the CellRanger's (version 4.0.0) cellranger multi command, combining GEX, VDJ, and antibody capture hashtag libraries. The command was run using Cell Ranger's supplied VDJ and GEX reference files, refdata-cellranger-vdj-GRCm38-alts-ensembl-4.0.0 and refdata-gex-mm10-2020-A.

Gene expression data was imported using the *scanpy* package in Python for two rounds of sequencing. Any cell whose second largest hashtag read count was at least 75% of the largest hashtag read count was filtered out. The remaining cells were assigned to their donor mice using the hashtag with the largest count value. Expression values were total sum scaled to 10,000 and then log normalized using a pseudocount of 1. $CD4^+$ and $CD8^+$ T cells were defined as cells expressing canonical T cell genes (*Cd3d* for example) and positive expression of either *Cd4* or *Cd8a*. Cells that had high expression of non-T cell genes or of both *Cd4* and *Cd8a* were excluded from subsequent analyses.

VDJ data were integrated into the single cell expression data using the *scirpy* package in Python. Only cells with high confidence VDJ calls containing a single productive rearrangement were retained. We then identified expanded CDR3α alpha and CDR3β sequences within $CD4^+$ and $CD8^+$ subsets by identifying sequences found in three or more cells within at least one mouse. Chi-squared tests were used to identify sequences with significantly different enrichment proportions between HC and HC+4% Gluten. The distributions of all expanded sequence clone sizes were then visualized using the *seaborn* package in Python. Clonotype clusters for CDR3α and CDR3β sequences were identified using pairwise alignment distance of the amino acid sequence using the BLOSUm62 scoring

matrix[77]. Clusters were identified using an arbitrary distance threshold of 5. The network of clonotype clusters was generated and visualized using *clonotype_network* from the *scirpy* package in Python.

Flow Cytometry—Single cell suspensions were incubated with Zombie Near IR (Biolegend, 423105) in 1X PBS for 10 minutes at room temperature for Live/Dead discrimination. Cells were then washed in 1X PBS supplemented with 1% FBS and 0.05% NaN_3. To block Fc receptors, cells were incubated in 1X PBS supplemented with 1% FBS and 0.05% NaN_3 and anti-mouse CD16/32 antibodies (Biolegend, 101301) for 10 minutes at 4° C. For surface staining, cells were incubated for 30 minutes at 4° C with fluorescently tagged antibodies. For analysis of islet infiltrates, cells were stained with α-CD45 (30-F11), -CD4 (GK1.5), -CD19 (1D3), -FR4 (12A5), -PD-L1 (MIH5), -CD62L (MEL-14), -CD80 (16-10A1), PD-1 (J43), and -CD11c (N418) all from BD Bioscience, and α-CD44 (IM7), -CD103 (2E7), -CD69 (H1.2F3), -CD11b (M1/70), -F4/80 (BM8), -CD86 (PO3), -TCRβ (H57-597), and -CD8α (53-6.7) all from Biolegend. For analysis of stimulated PLN macrophages, cells were stained with α-CD19 (1D3) from BD Bioscience, and α-CD11c (N418), -CD11b (M1/70), -F4/80 (BM8), and -TCRβ (H57-597) from Biolegend. Cells were then fixed and permeabilized using the Foxp3/Transcription Factor Staining Buffer Set (ThermoFisher) according to the manufacturer's instructions. Cells were then stained with fluorescently tagged intracellular antibodies overnight at 4° C. For analysis of islet infiltrates, cells were intracellularly stained with α-FoxP3 (FJK-16S) from Thermo/Fisher, α-CTLA-4 (UC10-4B9), and -Ki67 (16A8) from Biolegend, and α-Insulin (182410) from R&D Systems. For analysis of stimulated PLN macrophages, cells were intracellularly stained with α-TNFα (MP6-XT22) from Biolegend. Flow cytometry on islet infiltrates and stimulated pancreatic lymph node macrophages was done on a Cytek Aurora Instrument (Cytek). Raw data was unmixed using single color controls made using UltraComp ebeads™ Compensation beads (ThermoFisher) prepared according to the manufacturer's instructions or cells. Data was analyzed using FlowJo software (Treestar) with the UMAP plugin[78]

Western blotting was performed using thymic lysates in RIPA buffer (Stem—Cell Technology) supplemented with protease inhibitor cocktail (Pierce Thermo-Fisher) and separated by gel electrophoresis (20μg of protein/lane). Blots were stained with anti-TGM2 primary antibodies (R&D Systems,) or mouse anti-actin (clone C4, Santa Cruz Biotechnology) followed by secondary HRP-anti-sheep Ig conjugate (R&D Systems) or by HRP-sheep-anti-mouse-Ig conjugate (Amersham) respectively and developed using Super Signal West Femto Maximum Sensitivity Substrate (Thermo-Fisher).

Bacterial DNA sequencing and analysis—Small intestine and cecal contents of female mice were collected using sterile instruments into cryovials and snap frozen in liquid nitrogen until processing. Samples were processed and sequenced at the Environmental Sample Preparation and Sequencing Facility at Argonne National Laboratory. DNA was extracted from the samples using the DNeasy PowerSoil HTP 96 Kit (QIAGEN, Germantown, MD) according to the manufacturer's instructions. The V4 region of the 16S rRNA-encoding gene (515F-806R) was PCR amplified to survey the total bacterial community in the extracted samples using the Illumina MiSeq platform as described [79,80].

PCR reactions were carried out in triplicate for each sample using sterile, DNase-free 96 well plates with appropriate (DNA template-free) negative controls using the 5 PRIME MasterMix (5 PRIME, Gaithersburg, MD). PCR reactions were conducted using an initial denaturation step of 95°C for 3 minutes, followed by 35 cycles at 95°C for 30 seconds, 55°C for 45 seconds, then 72°C for 1.5 minutes. A single extension step at 72°C for 10 minutes was used at the end. Triplicate PCR reactions were then pooled together, primer dimers were removed from the pooled products using the UltraClean 96 PCR Cleanup Kit (QIAGEN) and total DNA quantified using the PicoGreen® dsDNA Assay (Life Technologies) was resuspended at 2 ng/μl. Amplicons were sequenced on an Illumina MiSeq using 151×151 base pair paired-end sequencing. Raw sequence data was processed using the QIIME 1.9 analysis pipeline [81]. Initially, paired-end reads were joined and then aligned to a database of reference sequences using PyNAST[82]. These were clustered into operational taxonomic units (OTUs) using UCLUST at 97% similarity [83] and a consensus taxonomy from the Greengenes reference database [84] was assigned to each sequence using the UCLUST taxonomy assigner.

Statistical analysis of the 16S dataset was carried out with the MATLAB (MathWorks, Natick, MA, USA) software package. Principal component analysis (PCA) of the microbiomes was performed using the relative abundance of genera from each sample. The percent variance explained by each principal component was calculated and reported in corresponding figures. Genera with the highest relative abundance were identified based on mean expression across all mice in small intestine and cecum. The top ten genera were visualized using a box plot to demonstrate differences among diets.

Detection of gluten-digesting bacteria—Serial 10-fold dilutions (from 10^{-3} to 10^{-7}) of mouse small intestine contents were plated on BHI-gliadin agar plates (Sigma) and on minimal medium-gluten agar plates[85] and the plates were incubated anaerobically for 2 – 6 days at 37°C. Gliadin-digesting colonies were detected by transparent halos formed around them in the cloudy gliadin-agar layer[86]. Colonies with transparent halos were then subcultured onto agar plates supplemented with gliadin ethanol extracts to confirm enzymatic activity. For identification of bacteria, DNA was extracted from individual colonies and 16S rDNA amplified and analyzed by Sanger sequencing.

Preparation of Gluten Digests—Gluten powder (3%, w/vol) was suspended in the appropriate liquid phase: BHI, Dulbecco's Modification of Eagle's medium (DMEM, Gibco), or bacterial culture supernatants grown in the above media. When required, 1% by volume of the log phase bacterial culture was added to the mix. The samples were incubated at 37°C for 18-20 hours with sufficient shaking to maintain gluten particles in suspension. Samples were then centrifuged to precipitate the non-soluble matter, filter-sterilized with 0.22um membrane filters and frozen at −80°C. Resulting supernatants were used for further analysis. For heat inactivation experiments, samples were incubated at 85°C for 30 minutes. For trypsin experiments, trypsin-EDTA (Gibco) was applied to the samples at a final concentration of 0.05% and samples were subsequently incubated overnight at 37°C. For polymyxin B treatment, 100 μL of polymyxin B-Agarose beads (Sigma) per ml of sample were incubated with prepared supernatants at 4°C overnight with gentle rotation. Beads

were removed by centrifugation at 800g for 10 minutes followed by passing the supernatant through a 0.22um membrane filter.

Activation of gliadin-specific T cells in vitro—Mouse T cell line 578_BV7_AV12 and TCC489_2_1_4 were made by engineering murine BW58α-β cells devoid of endogenous TCR to express human CD4 and TCR from a DQ2.5- glia-ω2–reactive CD4 T cell clone (TCC 578) or a DQ8-glia-α1-reactive CD4 T cell clone (TCC 489) as previously described[40,87]. IL-2 secretion was measured after overnight incubation of $5x10^4$ T cells with $5\text{-}10x10^3$ human lymphoblastoid cell line expressing HLA-DQ2.5 (a generous gift from Dr. Carole Ober, The University of Chicago) in 200μl of Click's medium with 5% fetal calf serum. IL2-secretion was elicited by addition of 10% (v/v) or less of bacterial digests of wheat gluten. IL-2 levels were determined by ELISA using a kit (Biolegend) according to manufacturer's instructions.

Stimulation of macrophages with gluten digests—Peritoneal macrophages were isolated 4 days after intraperitoneal administration of 1.5 ml of Thioglycolate (Difco). Macrophages were plated in Click's medium at 10^5 cells per well in a 96 well flat-bottom plate. Sterile filtered supernatants prepared as above were applied to the macrophages at a maximal concentration of 10% of the final culture volume unless specified otherwise. Supernatants were collected at hour 6 to assay TNF production and after overnight culture (18-20) hours to assay IL-6 production. TNF and IL-6 were measured using ELISA kits (BD and Biolegend) according to the manufacturers' instructions.

Stimulation of Pancreatic Lymph Node Macrophages—Pancreatic lymph nodes from 6–10-week-old NOD mice were incubated with Collagenase D (1.78 mg/ml, Roche 11088858001) and DNase I (0.1 mg/ml, Sigma DN25) in Click's media with 10% FBS for 30 minutes at 37° C and then passed through a nylon mesh to release macrophages. Single cell suspensions were then plated at 10^6 cells per well of a non-TC treated, round bottom 96 well plate and incubated for 6 hours with GolgiPlug only (1:500 vol/vol, BD555029), GolgiPlug and *E. faecalis* gluten digest (10% final culture volume), or GolgiPlug and 1 ng/ml of LPS. Cells were then washed and stained with fluorescently labeled antibodies.

Limulus amebocyte lysate (LAL) assay—LPS concentrations were determined with kinetic-chromogenic test kit Endochrome-K (Charles River Endosafe, Charleston, SC) according to the manufacturer's protocol. All reagents and components used for the assay were endotoxin-free. The LAL Reagent was rehydrated with Endotoxin-Specific Buffer Solution to prevent interference of β-D-Glucans with LAL-reactive material during testing. *E. coli* Control Standard Endotoxin (Charles River Endosafe) was used for the standard calibration curve dilutions. Test samples were incubated overnight at 30mg/ml of DMEM 37°C with constant shaking. Insoluble material was removed by centrifugation and 0.1 ml of each sample was transferred in a well of a LAL test-certified 96-well microplate (Greiner Bio-One GmbH, Frickenhausen, Germany). 0.1 ml of LAL reagent was quickly added to each well. The contents of the wells were mixed by tapping and the plate was placed in the VERSAmax microplate reader (Molecular Devices, Sunnyvale, CA). The 450 nm absorbance values were recorded for each well every 15s for 1 hour at room temperature.

Onset times at 0.200 OD units were used to calculate the LPS standard curve and the sample LPS concentration.

Quantification and Statistical Analysis

Statistical analysis of diabetes incidence, cell proliferation, blood glucose levels, flow cytometry, and ELISA results were performed using Prism 9 (GraphPad). All bar-graphs and dot-plots are expressed as Means ± sem. The statistical difference between any two groups was determined by Student's t test. For multiple groups the statistical difference was determined using the one-way analysis of variance (ANOVA) with post-hoc Tukey test. Statistics for T1D survival data were determined by Mantel-Cox long-rank test using Prism 9 (GraphPad). Incremental Area Under the Curve (iAUC) for IPGTT results were calculated in Prism 9 from curves drawn from the difference in glucose levels at each timepoint and time 0. p-values or adjusted p-values < 0.05 were considered statistically significant.

Supplementary Material

Refer to Web version on PubMed Central for supplementary material.

Acknowledgments

The authors are grateful to Grace Ryan, Brandon Hawkins and Laura Sams for their assistance with experiments, to Sarah Owens and the staff of the Environmental Sample Preparation and Sequencing Facility at Argonne National Laboratory for their assistance, to Genetic Engineering Technologies Core group at the Jackson Laboratory for assistance in generating Tgm2 KO mice, to Barbara Mickelson of Envigo for help with diet formulations, to Drs. Barbara Murray and Kavindra Singh for the mutant strain TX5243 and for valuable advice, to Dr. Michael Fischbach for his kind gift of penta-acylated LPS and to Dr. Joseph Pickard for critical reading of the manuscript.

LAY was supported by NIH T32 GM007183. CHFH was supported in part by Carlsberg Foundation, Denmark. L.M.S and S.D-K were supported by South-Eastern Norway Regional Health Authority (project number 2015009). DS was supported by grants DK46266, DK95735 and OD-020351. AVC was supported by NIH grants R01AI082418, R21AI115683, R01AI158744, DOD grant W911NF-17-1-0402 and a grant SRA-2015-8-Q-R from Juvenile Diabetes Research Foundation. This work was also supported by NIH/NIDDK Digestive Disease Research Core Center grant DK42086. The graphical abstract was created with BioRender.com.

References

1. Bach JF (2018). The hygiene hypothesis in autoimmunity: the role of pathogens and commensals. Nat Rev Immunol 18, 105–120. 10.1038/nri.2017.111. [PubMed: 29034905]
2. Norris JM, Johnson RK, and Stene LC (2020). Type 1 diabetes-early life origins and changing epidemiology. Lancet Diabetes Endocrinol 8, 226–238. 10.1016/S2213-8587(19)30412-7. [PubMed: 31999944]
3. Knip M, and Siljander H (2016). The role of the intestinal microbiota in type 1 diabetes mellitus. Nat Rev Endocrinol 12, 154–167. 10.1038/nrendo.2015.218. [PubMed: 26729037]
4. Lefebvre DE, Powell KL, Strom A, and Scott FW (2006). Dietary proteins as environmental modifiers of type 1 diabetes mellitus. Annu Rev Nutr 26, 175–202. 10.1146/annurev.nutr.26.061505.111206. [PubMed: 16848704]
5. Scott FW (1996). Food-induced type 1 diabetes in the BB rat. Diabetes Metab Rev 12, 341–359. 10.1002/(SICI)1099-0895(199612)12:4<341::AID-DMR173>3.0.CO;2-O. [PubMed: 9013075]
6. Coleman DL, Kuzava JE, and Leiter EH (1990). Effect of diet on incidence of diabetes in nonobese diabetic mice. Diabetes 39, 432–436. [PubMed: 2318346]
7. Lamb MM, Frederiksen B, Seifert JA, Kroehl M, Rewers M, and Norris JM (2015). Sugar intake is associated with progression from islet autoimmunity to type 1 diabetes: the Diabetes

Autoimmunity Study in the Young. Diabetologia 58, 2027–2034. 10.1007/s00125-015-3657-x. [PubMed: 26048237]

8. Lamb MM, Miller M, Seifert JA, Frederiksen B, Kroehl M, Rewers M, and Norris JM (2015). The effect of childhood cow's milk intake and HLA-DR genotype on risk of islet autoimmunity and type 1 diabetes: the Diabetes Autoimmunity Study in the Young. Pediatr Diabetes 16, 31–38. 10.1111/pedi.12115. [PubMed: 24444005]
9. Hakola L, Miettinen ME, Syrjala E, Akerlund M, Takkinen HM, Korhonen TE, Ahonen S, Ilonen J, Toppari J, Veijola R, et al. (2019). Association of Cereal, Gluten, and Dietary Fiber Intake With Islet Autoimmunity and Type 1 Diabetes. JAMA Pediatr. 10.1001/jamapediatrics.2019.2564.
10. Wen L, Ley RE, Volchkov PY, Stranges PB, Avanesyan L, Stonebraker AC, Hu C, Wong FS, Szot GL, Bluestone JA, et al. (2008). Innate immunity and intestinal microbiota in the development of Type 1 diabetes. Nature 455, 1109–1113. nature07336 [pii] 10.1038/nature07336. [PubMed: 18806780]
11. Vatanen T, Franzosa EA, Schwager R, Tripathi S, Arthur TD, Vehik K, Lernmark A, Hagopian WA, Rewers MJ, She JX, et al. (2018). The human gut microbiome in early-onset type 1 diabetes from the TEDDY study. Nature 562, 589–594. 10.1038/s41586-018-0620-2. [PubMed: 30356183]
12. Wu HJ, Ivanov II, Darce J, Hattori K, Shima T, Umesaki Y, Littman DR, Benoist C, and Mathis D (2010). Gut-residing segmented filamentous bacteria drive autoimmune arthritis via T helper 17 cells. Immunity 32, 815–827. S1074-7613(10)00204-9 [pii] 10.1016/j.immuni.2010.06.001. [PubMed: 20620945]
13. David LA, Materna AC, Friedman J, Campos-Baptista MI, Blackburn MC, Perrotta A, Erdman SE, and Alm EJ (2014). Host lifestyle affects human microbiota on daily timescales. Genome Biol 15, R89. 10.1186/gb-2014-15-7-r89. [PubMed: 25146375]
14. Faith JJ, McNulty NP, Rey FE, and Gordon JI (2011). Predicting a human gut microbiota's response to diet in gnotobiotic mice. Science 333, 101–104. 10.1126/science.1206025. [PubMed: 21596954]
15. Carmody RN, Gerber GK, Luevano JM Jr., Gatti DM, Somes L, Svenson KL, and Turnbaugh PJ (2015). Diet dominates host genotype in shaping the murine gut microbiota. Cell Host Microbe 17, 72–84. 10.1016/j.chom.2014.11.010. [PubMed: 25532804]
16. Krautkramer KA, Kreznar JH, Romano KA, Vivas EI, Barrett-Wilt GA, Rabaglia ME, Keller MP, Attie AD, Rey FE, and Denu JM (2016). Diet-Microbiota Interactions Mediate Global Epigenetic Programming in Multiple Host Tissues. Mol Cell 64, 982–992. 10.1016/j.molcel.2016.10.025. [PubMed: 27889451]
17. Schroeder BO, and Backhed F (2016). Signals from the gut microbiota to distant organs in physiology and disease. Nat Med 22, 1079–1089. 10.1038/nm.4185. [PubMed: 27711063]
18. Human Microbiome Project C (2012). Structure, function and diversity of the healthy human microbiome. Nature 486, 207–214. 10.1038/nature11234. [PubMed: 22699609]
19. Gilbert JA, Blaser MJ, Caporaso JG, Jansson JK, Lynch SV, and Knight R (2018). Current understanding of the human microbiome. Nat Med 24, 392–400. 10.1038/nm.4517. [PubMed: 29634682]
20. Elliott RB, Reddy SN, Bibby NJ, and Kida K (1988). Dietary prevention of diabetes in the non-obese diabetic mouse. Diabetologia 31, 62–64. [PubMed: 3280372]
21. Beales PE, Elliott RB, Flohe S, Hill JP, Kolb H, Pozzilli P, Wang GS, Wasmuth H, and Scott FW (2002). A multi-centre, blinded international trial of the effect of A(1) and A(2) beta-casein variants on diabetes incidence in two rodent models of spontaneous Type I diabetes. Diabetologia 45, 1240–1246. 10.1007/s00125-002-0898-2. [PubMed: 12242456]
22. Patrick C, Wang GS, Lefebvre DE, Crookshank JA, Sonier B, Eberhard C, Mojibian M, Kennedy CR, Brooks SP, Kalmokoff ML, et al. (2013). Promotion of autoimmune diabetes by cereal diet in the presence or absence of microbes associated with gut immune activation, regulatory imbalance, and altered cathelicidin antimicrobial Peptide. Diabetes 62, 2036–2047. 10.2337/db12-1243. [PubMed: 23349499]
23. Katz JD, Benoist C, and Mathis D (1995). T helper cell subsets in insulin-dependent diabetes. Science 268, 1185–1188. [PubMed: 7761837]

24. Nakayama M, Abiru N, Moriyama H, Babaya N, Liu E, Miao D, Yu L, Wegmann DR, Hutton JC, Elliott JF, and Eisenbarth GS (2005). Prime role for an insulin epitope in the development of type 1 diabetes in NOD mice. Nature 435, 220–223. [PubMed: 15889095]
25. Chaparro RJ, Konigshofer Y, Beilhack GF, Shizuru JA, McDevitt HO, and Chien YH (2006). Nonobese diabetic mice express aspects of both type 1 and type 2 diabetes. Proc Natl Acad Sci U S A 103, 12475–12480. 10.1073/pnas.0604317103. [PubMed: 16895987]
26. Liston A, Todd JA, and Lagou V (2017). Beta-Cell Fragility As a Common Underlying Risk Factor in Type 1 and Type 2 Diabetes. Trends Mol Med 23, 181–194. 10.1016/j.molmed.2016.12.005. [PubMed: 28117227]
27. Sildorf SM, Fredheim S, Svensson J, and Buschard K (2012). Remission without insulin therapy on gluten-free diet in a 6-year old boy with type 1 diabetes mellitus. BMJ Case Rep 2012. 10.1136/bcr.02.2012.5878.
28. Mootha VK, Lindgren CM, Eriksson KF, Subramanian A, Sihag S, Lehar J, Puigserver P, Carlsson E, Ridderstrale M, Laurila E, et al. (2003). PGC-1alpha-responsive genes involved in oxidative phosphorylation are coordinately downregulated in human diabetes. Nat Genet 34, 267–273. 10.1038/ng1180. [PubMed: 12808457]
29. Subramanian A, Tamayo P, Mootha VK, Mukherjee S, Ebert BL, Gillette MA, Paulovich A, Pomeroy SL, Golub TR, Lander ES, and Mesirov JP (2005). Gene set enrichment analysis: a knowledge-based approach for interpreting genome-wide expression profiles. Proc Natl Acad Sci U S A 102, 15545–15550. 10.1073/pnas.0506580102. [PubMed: 16199517]
30. Miragaia RJ, Gomes T, Chomka A, Jardine L, Riedel A, Hegazy AN, Whibley N, Tucci A, Chen X, Lindeman I, et al. (2019). Single-Cell Transcriptomics of Regulatory T Cells Reveals Trajectories of Tissue Adaptation. Immunity 50, 493–504 e497. 10.1016/j.immuni.2019.01.001. [PubMed: 30737144]
31. Spence A, Purtha W, Tam J, Dong S, Kim Y, Ju CH, Sterling T, Nakayama M, Robinson WH, Bluestone JA, et al. (2018). Revealing the specificity of regulatory T cells in murine autoimmune diabetes. Proc Natl Acad Sci U S A 115, 5265–5270. 10.1073/pnas.1715590115. [PubMed: 29712852]
32. Delacher M, Imbusch CD, Hotz-Wagenblatt A, Mallm JP, Bauer K, Simon M, Riegel D, Rendeiro AF, Bittner S, Sanderink L, et al. (2020). Precursors for Nonlymphoid-Tissue Treg Cells Reside in Secondary Lymphoid Organs and Are Programmed by the Transcription Factor BATF. Immunity 52, 295–312 e211. 10.1016/j.immuni.2019.12.002. [PubMed: 31924477]
33. Santamaria P, Utsugi T, Park BJ, Averill N, Kawazu S, and Yoon JW (1995). Beta-cell-cytotoxic CD8+ T cells from nonobese diabetic mice use highly homologous T cell receptor alpha-chain CDR3 sequences. J Immunol 154, 2494–2503. [PubMed: 7868915]
34. Verdaguer J, Schmidt D, Amrani A, Anderson B, Averill N, and Santamaria P (1997). Spontaneous autoimmune diabetes in monoclonal T cell nonobese diabetic mice. J Exp Med 186, 1663–1676. [PubMed: 9362527]
35. DiLorenzo TP, Graser RT, Ono T, Christianson GJ, Chapman HD, Roopenian DC, Nathenson SG, and Serreze DV (1998). Major histocompatibility complex class I-restricted T cells are required for all but the end stages of diabetes development in nonobese diabetic mice and use a prevalent T cell receptor alpha chain gene rearrangement. Proc Natl Acad Sci U S A 95, 12538–12543. 10.1073/pnas.95.21.12538. [PubMed: 9770521]
36. Sollid LM, and Jabri B (2013). Triggers and drivers of autoimmunity: lessons from coeliac disease. Nat Rev Immunol 13, 294–302. 10.1038/nri3407. [PubMed: 23493116]
37. Khan AA, Yurkovetskiy L, O'Grady K, Pickard JM, de Pooter R, Antonopoulos DA, Golovkina T, and Chervonsky A (2019). Polymorphic Immune Mechanisms Regulate Commensal Repertoire. Cell Rep 29, 541–550 e544. 10.1016/j.celrep.2019.09.010. [PubMed: 31618625]
38. Urade R, Sato N, and Sugiyama M (2018). Gliadins from wheat grain: an overview, from primary structure to nanostructures of aggregates. Biophys Rev 10, 435–443. 10.1007/s12551-017-0367-2. [PubMed: 29204878]
39. Dahal-Koirala S, Risnes LF, Christophersen A, Sarna VK, Lundin KE, Sollid LM, and Qiao SW (2016). TCR sequencing of single cells reactive to DQ2.5-glia-alpha2 and DQ2.5-glia-omega2 reveals clonal expansion and epitope-specific V-gene usage. Mucosal Immunol 9, 587–596. 10.1038/mi.2015.147. [PubMed: 26838051]

40. Qiao SW, Raki M, Gunnarsen KS, Loset GA, Lundin KE, Sandlie I, and Sollid LM (2011). Posttranslational modification of gluten shapes TCR usage in celiac disease. J Immunol 187, 3064–3071. 10.4049/jimmunol.1101526. [PubMed: 21849672]
41. Sifri CD, Mylonakis E, Singh KV, Qin X, Garsin DA, Murray BE, Ausubel FM, and Calderwood SB (2002). Virulence effect of Enterococcus faecalis protease genes and the quorum-sensing locus fsr in Caenorhabditis elegans and mice. Infect Immun 70, 5647–5650. 10.1128/IAI.70.10.5647-5650.2002. [PubMed: 12228293]
42. Singh KV, Qin X, Weinstock GM, and Murray BE (1998). Generation and testing of mutants of Enterococcus faecalis in a mouse peritonitis model. J Infect Dis 178, 1416–1420. 10.1086/314453. [PubMed: 9780263]
43. Kawalec M, Potempa J, Moon JL, Travis J, and Murray BE (2005). Molecular diversity of a putative virulence factor: purification and characterization of isoforms of an extracellular serine glutamyl endopeptidase of Enterococcus faecalis with different enzymatic activities. J Bacteriol 187, 266–275. 10.1128/JB.187.1.266-275.2005. [PubMed: 15601711]
44. Murray BE, Singh KV, Ross RP, Heath JD, Dunny GM, and Weinstock GM (1993). Generation of restriction map of Enterococcus faecalis OG1 and investigation of growth requirements and regions encoding biosynthetic function. J Bacteriol 175, 5216–5223. 10.1128/jb.175.16.5216-5223.1993. [PubMed: 8349561]
45. Qin X, Singh KV, Weinstock GM, and Murray BE (2001). Characterization of fsr, a regulator controlling expression of gelatinase and serine protease in Enterococcus faecalis OG1RF. J Bacteriol 183, 3372–3382. 10.1128/JB.183.11.3372-3382.2001. [PubMed: 11344145]
46. Burrows MP, Volchkov P, Kobayashi KS, and Chervonsky AV (2015). Microbiota regulates type 1 diabetes through Toll-like receptors. Proc Natl Acad Sci U S A 112, 9973–9977. 10.1073/pnas.1508740112. [PubMed: 26216961]
47. Yurkovetskiy LA, Pickard JM, and Chervonsky AV (2015). Microbiota and autoimmunity: exploring new avenues. Cell Host Microbe 17, 548–552. 10.1016/j.chom.2015.04.010. [PubMed: 25974297]
48. Freiesleben De Blasio B, Bak P, Pociot F, Karlsen AE, and Nerup J (1999). Onset of type 1 diabetes: a dynamical instability. Diabetes 48, 1677–1685. [PubMed: 10480594]
49. Korem Kohanim Y, Tendler A, Mayo A, Friedman N, and Alon U (2020). Endocrine Autoimmune Disease as a Fragility of Immune Surveillance against Hypersecreting Mutants. Immunity 52, 872–884 e875. 10.1016/j.immuni.2020.04.022. [PubMed: 32433950]
50. Savinov AY, Wong FS, Stonebraker AC, and Chervonsky AV (2003). Presentation of antigen by endothelial cells and chemoattraction are required for homing of insulin-specific CD8+ T cells. J Exp Med 197, 643–656. 10.1084/jem.20021378. [PubMed: 12615905]
51. Varndell IM, Lloyd RV, Wilson BS, and Polak JM (1985). Ultrastructural localization of chromogranin: a potential marker for the electron microscopical recognition of endocrine cell secretory granules. Histochem J 17, 981–992. 10.1007/BF01417947. [PubMed: 4066407]
52. Wasmeier C, and Hutton JC (1996). Molecular cloning of phogrin, a protein-tyrosine phosphatase homologue localized to insulin secretory granule membranes. J Biol Chem 271, 18161–18170. 10.1074/jbc.271.30.18161. [PubMed: 8663434]
53. Davidson HW, Wenzlau JM, and O'Brien RM (2014). Zinc transporter 8 (ZnT8) and beta cell function. Trends Endocrinol Metab 25, 415–424. 10.1016/j.tem.2014.03.008. [PubMed: 24751356]
54. Knip M, Virtanen SM, Seppa K, Ilonen J, Savilahti E, Vaarala O, Reunanen A, Teramo K, Hamalainen AM, Paronen J, et al. (2010). Dietary Intervention in Infancy and Later Signs of Beta-Cell Autoimmunity. N Engl J Med 363, 1900–1908. 10.1056/NEJMoa1004809. [PubMed: 21067382]
55. Craig ME, Prinz N, Boyle CT, Campbell FM, Jones TW, Hofer SE, Simmons JH, Holman N, Tham E, Frohlich-Reiterer E, et al. (2017). Prevalence of Celiac Disease in 52,721 Youth With Type 1 Diabetes: International Comparison Across Three Continents. Diabetes Care 40, 1034–1040. 10.2337/dc16-2508. [PubMed: 28546222]

56. Smyth DJ, Plagnol V, Walker NM, Cooper JD, Downes K, Yang JH, Howson JM, Stevens H, McManus R, Wijmenga C, et al. (2008). Shared and distinct genetic variants in type 1 diabetes and celiac disease. N Engl J Med 359, 2767–2777. 10.1056/NEJMoa0807917. [PubMed: 19073967]
57. Warshauer JT, Belk JA, Chan AY, Wang J, Gupta AR, Shi Q, Skartsis N, Peng Y, Phipps JD, Acenas D, et al. (2021). A human mutation in STAT3 promotes type 1 diabetes through a defect in CD8+ T cell tolerance. J Exp Med 218. 10.1084/jem.20210759.
58. Wilks J, Lien E, Jacobson AN, Fischbach MA, Qureshi N, Chervonsky AV, and Golovkina TV (2015). Mammalian Lipopolysaccharide Receptors Incorporated into the Retroviral Envelope Augment Virus Transmission. Cell Host Microbe 18, 456–462. 10.1016/j.chom.2015.09.005. [PubMed: 26468748]
59. Gao B, and Tsan MF (2003). Recombinant human heat shock protein 60 does not induce the release of tumor necrosis factor alpha from murine macrophages. J Biol Chem 278, 22523–22529. 10.1074/jbc.M303161200. [PubMed: 12686536]
60. Habich C, Kempe K, van der Zee R, Rumenapf R, Akiyama H, Kolb H, and Burkart V (2005). Heat shock protein 60: specific binding of lipopolysaccharide. J Immunol 174, 1298–1305. 10.4049/jimmunol.174.3.1298. [PubMed: 15661886]
61. Junker Y, Zeissig S, Kim SJ, Barisani D, Wieser H, Leffler DA, Zevallos V, Libermann TA, Dillon S, Freitag TL, et al. (2012). Wheat amylase trypsin inhibitors drive intestinal inflammation via activation of toll-like receptor 4. J Exp Med 209, 2395–2408. 10.1084/jem.20102660. [PubMed: 23209313]
62. Aumeunier A, Grela F, Ramadan A, Pham Van L, Bardel E, Gomez Alcala A, Jeannin P, Akira S, Bach JF, and Thieblemont N (2010). Systemic Toll-like receptor stimulation suppresses experimental allergic asthma and autoimmune diabetes in NOD mice. PLoS One 5, e11484. 10.1371/journal.pone.0011484. [PubMed: 20628601]
63. Kihl P, Krych L, Deng L, Kildemoes AO, Laigaard A, Hansen LH, Hansen CHF, Buschard K, Nielsen DS, and Hansen AK (2019). Oral LPS Dosing Induces Local Immunological Changes in the Pancreatic Lymph Nodes in Mice. J Diabetes Res 2019, 1649279. 10.1155/2019/1649279. [PubMed: 30956991]
64. Wei G, Tian N, Valery AC, Zhong Y, Schuppan D, and Helmerhorst EJ (2015). Identification of Pseudolysin (lasB) as an Aciduric Gluten-Degrading Enzyme with High Therapeutic Potential for Celiac Disease. The American journal of gastroenterology 110, 899–908. 10.1038/ajg.2015.97. [PubMed: 25895519]
65. Szklarczyk D, Franceschini A, Kuhn M, Simonovic M, Roth A, Minguez P, Doerks T, Stark M, Muller J, Bork P, et al. (2011). The STRING database in 2011: functional interaction networks of proteins, globally integrated and scored. Nucleic Acids Res 39, D561–568. 10.1093/nar/gkq973. [PubMed: 21045058]
66. Kane M, Case LK, Kopaskie K, Kozlova A, MacDearmid C, Chervonsky AV, and Golovkina TV (2011). Successful transmission of a retrovirus depends on the commensal microbiota. Science 334, 245–249. 10.1126/science.1210718. [PubMed: 21998394]
67. Kasarda DD (2013). Can an increase in celiac disease be attributed to an increase in the gluten content of wheat as a consequence of wheat breeding? J Agric Food Chem 61, 1155–1159. 10.1021/jf305122s. [PubMed: 23311690]
68. Kristich CJ, Chandler JR, and Dunny GM (2007). Development of a host-genotype-independent counterselectable marker and a high-frequency conjugative delivery system and their use in genetic analysis of Enterococcus faecalis. Plasmid 57, 131–144. 10.1016/j.plasmid.2006.08.003. [PubMed: 16996131]
69. Bryan EM, Bae T, Kleerebezem M, and Dunny GM (2000). Improved vectors for nisin-controlled expression in gram-positive bacteria. Plasmid 44, 183–190. 10.1006/plas.2000.1484. [PubMed: 10964628]
70. Waters CM, Antiporta MH, Murray BE, and Dunny GM (2003). Role of the Enterococcus faecalis GelE protease in determination of cellular chain length, supernatant pheromone levels, and degradation of fibrin and misfolded surface proteins. J Bacteriol 185, 3613–3623. 10.1128/JB.185.12.3613-3623.2003. [PubMed: 12775699]
71. Lieberman SM, Evans AM, Han B, Takaki T, Vinnitskaya Y, Caldwell JA, Serreze DV, Shabanowitz J, Hunt DF, Nathenson SG, et al. (2003). Identification of the beta cell antigen

targeted by a prevalent population of pathogenic CD8+ T cells in autoimmune diabetes. Proc Natl Acad Sci U S A 100, 8384–8388. 10.1073/pnas.0932778100. [PubMed: 12815107]

72. Takaki T, Lieberman SM, Holl TM, Han B, Santamaria P, Serreze DV, and DiLorenzo TP (2004). Requirement for both H-2Db and H-2Kd for the induction of diabetes by the promiscuous CD8+ T cell clonotype AI4. J Immunol 173, 2530–2541. [PubMed: 15294969]
73. Wong FS, Karttunen J, Dumont C, Wen L, Visintin I, Pilip IM, Shastri N, Pamer EG, and Janeway CA Jr. (1999). Identification of an MHC class I-restricted autoantigen in type 1 diabetes by screening an organ-specific cDNA library. Nat Med 5, 1026–1031. [PubMed: 10470079]
74. Zheng GX, Terry JM, Belgrader P, Ryvkin P, Bent ZW, Wilson R, Ziraldo SB, Wheeler TD, McDermott GP, Zhu J, et al. (2017). Massively parallel digital transcriptional profiling of single cells. Nat Commun 8, 14049. 10.1038/ncomms14049. [PubMed: 28091601]
75. Hao Y, Hao S, Andersen-Nissen E, Mauck WM 3rd, Zheng S, Butler A, Lee MJ, Wilk AJ, Darby C, Zager M, et al. (2021). Integrated analysis of multimodal single-cell data. Cell 184, 3573–3587 e3529. 10.1016/j.cell.2021.04.048. [PubMed: 34062119]
76. Wolf FA, Angerer P, and Theis FJ (2018). SCANPY: large-scale single-cell gene expression data analysis. Genome Biol 19, 15. 10.1186/s13059-017-1382-0. [PubMed: 29409532]
77. Henikoff S, and Henikoff JG (1992). Amino acid substitution matrices from protein blocks. Proc Natl Acad Sci U S A 89, 10915–10919. 10.1073/pnas.89.22.10915. [PubMed: 1438297]
78. McInnes L, Healy J & Melville J (2020). Uniform Manifold Approximation and Projection for Dimension Reduction. arXiv:1802.03426 [cs, stat]
79. Walters W, Hyde ER, Berg-Lyons D, Ackermann G, Humphrey G, Parada A, Gilbert JA, Jansson JK, Caporaso JG, Fuhrman JA, et al. (2016). Improved Bacterial 16S rRNA Gene (V4 and V4-5) and Fungal Internal Transcribed Spacer Marker Gene Primers for Microbial Community Surveys. mSystems 1. 10.1128/mSystems.00009-15.
80. Caporaso JG, Lauber CL, Walters WA, Berg-Lyons D, Huntley J, Fierer N, Owens SM, Betley J, Fraser L, Bauer M, et al. (2012). Ultra-high-throughput microbial community analysis on the Illumina HiSeq and MiSeq platforms. Isme Journal 6, 1621–1624. 10.1038/ismej.2012.8. [PubMed: 22402401]
81. Caporaso JG, Kuczynski J, Stombaugh J, Bittinger K, Bushman FD, Costello EK, Fierer N, Pena AG, Goodrich JK, Gordon JI, et al. (2010). QIIME allows analysis of high-throughput community sequencing data. Nature methods 7, 335–336. 10.1038/nmeth.f.303. [PubMed: 20383131]
82. Caporaso JG, Bittinger K, Bushman FD, DeSantis TZ, Andersen GL, and Knight R (2010). PyNAST: a flexible tool for aligning sequences to a template alignment. Bioinformatics 26, 266–267. 10.1093/bioinformatics/btp636. [PubMed: 19914921]
83. Edgar RC (2010). Search and clustering orders of magnitude faster than BLAST. Bioinformatics 26, 2460–2461. 10.1093/bioinformatics/btq461. [PubMed: 20709691]
84. McDonald D, Price MN, Goodrich J, Nawrocki EP, DeSantis TZ, Probst A, Andersen GL, Knight R, and Hugenholtz P (2012). An improved Greengenes taxonomy with explicit ranks for ecological and evolutionary analyses of bacteria and archaea. Isme Journal 6, 610–618. 10.1038/ismej.2011.139. [PubMed: 22134646]
85. Zamakhchari M, Wei G, Dewhirst F, Lee J, Schuppan D, Oppenheim FG, and Helmerhorst EJ (2011). Identification of Rothia bacteria as gluten-degrading natural colonizers of the upper gastro-intestinal tract. PLoS One 6, e24455. 10.1371/journal.pone.0024455. [PubMed: 21957450]
86. Berger M, Sarantopoulos C, Ongchangco D, Sry J, and Cesario T (2015). Rapid isolation of gluten-digesting bacteria from human stool and saliva by using gliadin-containing plates. Exp Biol Med (Maywood) 240, 917–924. 10.1177/1535370214564748. [PubMed: 25519429]
87. Sollid LM, Qiao SW, Anderson RP, Gianfrani C, and Koning F (2012). Nomenclature and listing of celiac disease relevant gluten T-cell epitopes restricted by HLA-DQ molecules. Immunogenetics 64, 455–460. 10.1007/s00251-012-0599-z. [PubMed: 22322673]

Highlights

- Casein-based diet reduces β-cell stress and type-1 diabetes independent of microbes
- Gluten reverses casein-mediated protection when commensal microbes are present
- *E. faecalis*-mediated proteolysis of gluten triggers enhancement of autoimmunity
- Proteolysis potentiates proinflammatory properties of LPS associated with gluten

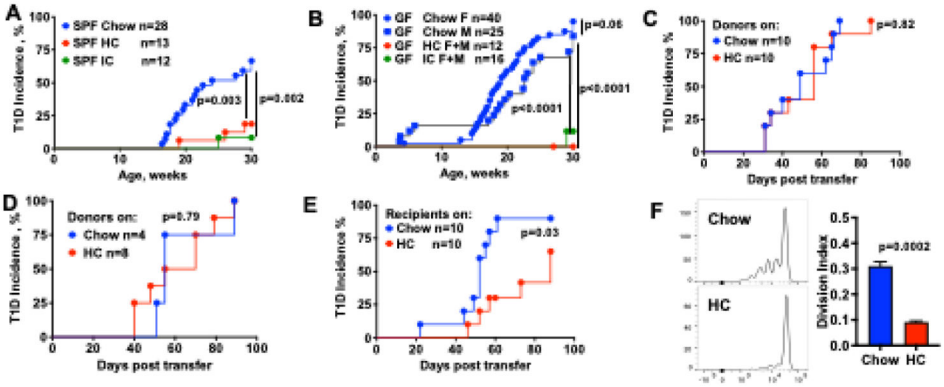

Figure 1. Protection from T1D by HC diet is independent from the microbiota

(A) Type 1 diabetes (T1D) incidence in SPF female NOD mice fed regular chow, hydrolyzed casein (HC), and intact casein (IC) diets.

(B) T1D in germ-free (GF) NOD mice on the same diets.

(C, **D)** Transfer of $2x10^7$ splenocytes from pre-diabetic SPF NOD mice fed either chow or HC into NOD.scid (**C**) or NOD.TCRα KO (**D**) recipients fed regular chow (data combined from 2 experiments).

(E) Transfer of $2x10^7$ splenocytes from SPF NOD mouse fed regular chow into NOD TCRα KO mice either on chow or HC diets (data combined from 2 experiments).

p values in **A**-**E** were estimated using Mantel-Cox long-rank test.

(F) Proliferation of CFSE-labeled BDC2.5 T cells 3 days after transfer in the pancreatic lymph nodes of recipient SPF NOD mice fed chow or HC diets (representative experiment of 3 independent experiments, three mice per group). Mean±sem. *p* value calculated using Student's *t* test.

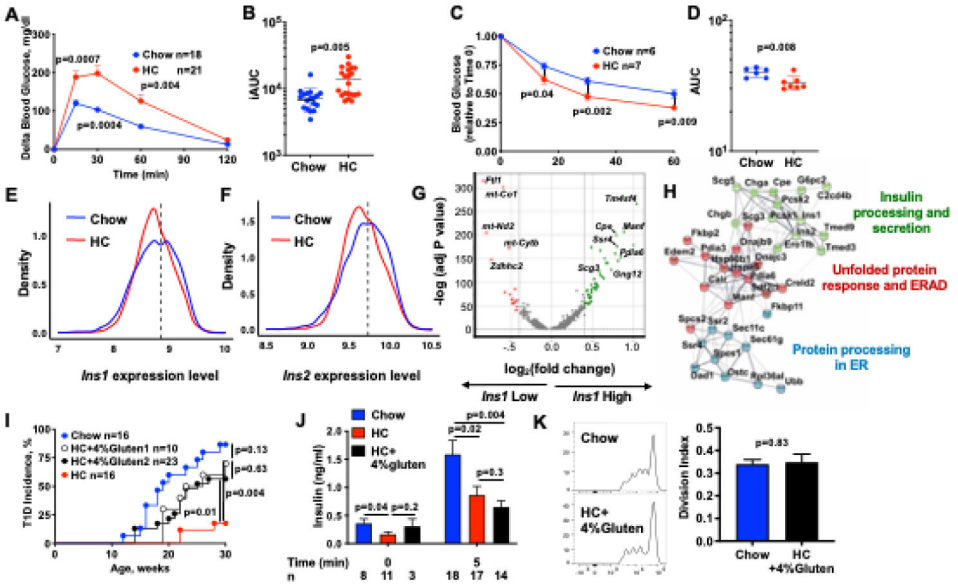

Figure 2. Effects of HC and HC+4%gluten diets on insulin secretion

(A, B) Intraperitoneal Glucose Tolerance Test (IPGTT) performed on 6–8-week-old NOD female mice either fed chow or HC diets shown as **(A)** the change of blood glucose levels after subtraction of the zero-time-point for every mouse (delta) and **(B)** calculation of Incremental Area Under the Curve (iAUC) for the same experiments. Combined data from 5 independent experiments, mean±sem. *p* values were calculated using Student's *t* test. n=number of animals per group.

(C, **D**) Test for insulin resistance – (**C**) blood glucose clearance in 6–8-week-old mice fed indicated diets and injected with insulin after 6 hrs fasting and **(D)** AUC calculated for the same experiments. Combined data from two experiments, mean±sem. *p* values calculated using Student's *t* test. n=number of animals per group.

(E, **F)** Distribution of relative *Ins1* and *Ins2* gene expression levels in β-cells from 8–10-week-old NOD.scid mice fed regular chow (blue line) or HC diet (red line). Data is based on single-cell RNA sequencing (SCS) of NOD.scid islets and is plotted as a kernel density estimation function. Dashed vertical line indicates the border between low and high expressors of insulin in islets of chow fed mice. The *p* values calculated by Mann-Whitney U test were $4.9x10^{-1}$ and $1.4x10^{-14}$ for *Ins 1* and *Ins 2*, respectively.

(G) Volcano plot showing differential gene expression between *Ins1*-High and *Ins1*-Low beta cells isolated from the islets of NOD.scid mice fed regular chow. Genes indicated have adjusted p-values less than 0.05 and log2 fold change magnitude greater than 0.5.

(H) Gene networks built using genes upregulated in β-cells with high insulin expression compared to β-cells with low insulin expression using STRING database [65].

(I) Glutens from two different manufacturers were added to HC diet replacing 1/5th of hydrolyzed casein weight (or 4% of the total diet weight, thus termed 'HC−4%gluten diet') and T1D incidence in female NOD mice was observed in the same experiment.

(J) Direct measurements of plasma insulin in NOD mice fed chow, HC, or HC+4%gluten at fasting baseline and 5 minutes after glucose challenge. Mean±sem. *p* values were calculated using Student's *t* test.

(K) Proliferation of CFSE-labeled BDC2.5 T cells in the pancreatic lymph nodes of mice on chow and HC+4%gluten diets. Mean±sem. Combined data from 2 experiments, *p* value was calculated using Student's *t* test.

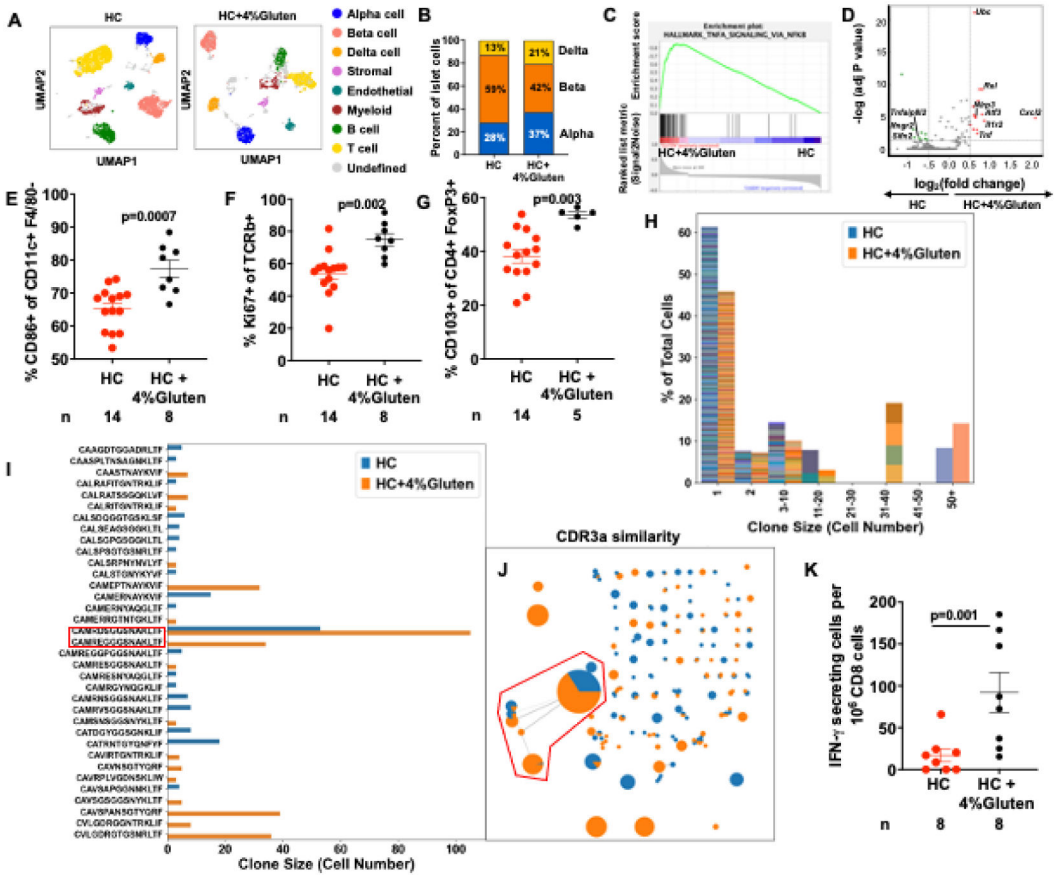

Figure 3. Gluten promotes immune activation in pancreatic islets.

(A) Uniform Manifold Approximation and Projection (UMAP) dimension reduction plots of islet cells from 15-week-old NOD mice on indicated diets (SCS analysis, pool of 3 mice per group).

(B) Ratios of α-, β-, and *δ*-cells in the islets of HC− and HC + 4%gluten-fed NOD mice defined by SCS.

(C) Gene Set Enrichment Analysis (GSEA) showing enrichment of hallmark TNFα signaling via NFκB in β-cells from HC+4%gluten fed NOD islets. FDR q value <0.05.

(D) Volcano plot showing differential gene expression between myeloid cells from islets of HC and HC+4%gluten fed NOD mice. Genes indicated have adjusted *p* values less than 0.05 and log2 fold change magnitude greater than 0.5.

(E) Quantification of CD86 expression by dendritic cells ($CD45^+$ $CD11c^+$ $F4/80^-$) in the islets of HC and HC+4%gluten fed NOD mice. Data combined from 6 experiments. Mean±sem. *p* value was calculated using Student's *t* test.

(F) Quantification of Ki67 expression in αβ T cells ($CD45^+$, $CD11c^-$, $F4/80^-$, $CD19^+$, $TCR\beta^+$) from the islets of HC and HC+4%gluten fed NOD mice. Data combined from 6 experiments. Mean±sem. *p* value was calculated using Student's *t* test.

(G) Quantification of CD103 expression in Tregs ($CD45^+$, $CD11c^-$, $F4/80^-$, $CD19^-$, $TCR\beta^+$, $CD4^+$, $FoxP3^+$) from the islets of HC and HC+4%gluten fed NOD mice. Data combined from 6 experiments. Mean±sem. *p* value was calculated using Student's *t* test.

(H) Distribution of expanded CDR3α sequences and clonal sizes in islet infiltrates from mice on HC (blue background) and HC+4%Gluten (orange background) diets from single cell sequenced $CD8^+$ cells (three mice per diet). The abscissa represents the size of expanded clonotypes and the ordinate represents the % of individual clonotype of total sequenced $CD8^+$ cells. Individual CDR3α sequences are represented by different colors.
(I) The number of expanded cells from each clonotype (≥3 cells with identical TCRs) derived from expanded CDR3α sequences from $CD8^+$ cells in the islets of HC (blue) and HC+4%Gluten (orange) fed mice. CDR3α identical and visibly similar to NY8.3 are highlighted with a red rectangle.
(J) Network of clonotype clusters derived from pairwise sequence alignment of CDR3α sequences for $CD8^+$ cells. Each circle represents a unique CDR3α sequence and the size of the circle is proportional to the size of the clone. Dashed lines represent clusters of sequences whose distance was within a similarity score of 5 based on BLOSUM62 scoring. Clonotypes carrying CDR3α identical or similar to NY8.3 are highlighted with a red line.
(K) The frequency of CD8+ T cells producing IFN-γ in response to NRPA7 mimic peptide recognized by the diabetogenic clone NY8.3 in the PLN from HC fed and HC+4%gluten fed NOD mice. Each point is an average of 3 technical replicates per mouse. Mean±sem. Data are combined from 3 experiments. *p* values calculated using Student's *t* test.

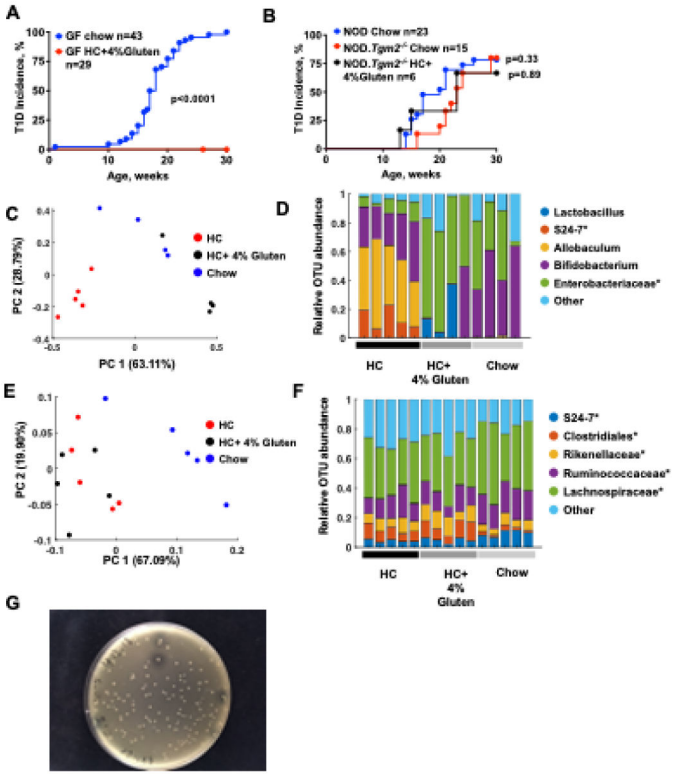

Figure 4. Enhancement of autoimmunity by gluten requires the microbiota

(A) Comparison of T1D incidence in GF mice fed chow or HC+4%gluten diet. n=number of animals per group. *p* value was estimated using Mantel-Cox long-rank test. n = number of animals per group.

(B) T1D development in TGM2-deficient mice fed either chow or HC+4%gluten diets at The University of Chicago, *p* value was estimated using Mantel-Cox long-rank test. n = number of animals per group.

(C), Principal Component Analysis of the small intestine (SI) microbiota of ex-GF mice simultaneously colonized with a single source of SPF NOD microbiota 8 weeks prior.

(D) Relative abundance of the top Operational Taxonomic Units (OTUs) in the SI microbiota of ex-GF mice fed indicated diets.

(E) Principal Component Analysis of the cecal microbiota of ex-GF mice simultaneously colonized with a single source of SPF NOD microbiota 8 weeks prior.

(F) Relative abundance of the top Operational Taxonomic Units (OTUs) in the cecal microbiota of ex-GF mice fed indicated diets.

(G) Some bacteria from the small intestine of a NOD mouse plated on brain heart infusion (BHI) agar containing gliadin secrete proteases leaving transparent halos around colonies.

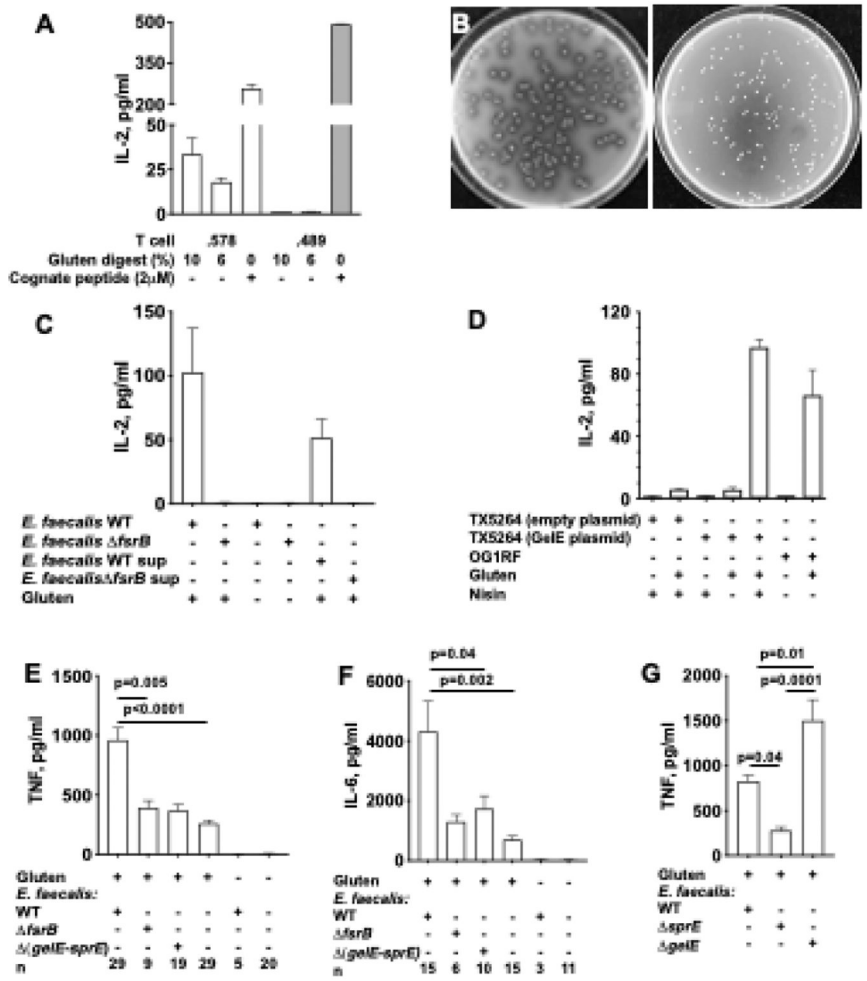

Figure 5. Gluten proteolysis by bacteria leads to activation of adaptive and innate immunity.

(A) Gluten digest by *E. faecalis* activates 578_BV7_AV12 (.578) T cells specific for glia-ω2 peptide/HLA-DQ2.5 but does not activate an independent T cell TCC489.2.14 (.489) specific for gliadin alpha1 peptide/HLA-DQ8 complex. Both T cells were readily activated by their cognate peptides. Mean±sem. Representative of two experiments.

(B) Digestion of gliadin by the wild-type *E. faecalis* strain OG1RF (left) and lack of digestion by Δ*fsrB* mutant TX5266 (right).

(C) IL-2 production by the .578 T cells in the presence of HLA-DQ2.5^{+} antigen-presenting cells and gluten digests performed overnight by indicated bacteria or by cell-free supernatants (sup) from the same bacteria. Mean±sem from a representative experiment out of 5 independent experiments.

(D) IL-2 production by the same T cells in the presence of APC and gluten digests produced by wild-type *E. faecalis* or mutant *gelE*-negative mutant TX5264 transformed with an empty control plasmid or a plasmid carrying *gelE* gene under nisin-sensitive promoter. Mean±sem from one out of 2 independent experiments.

(E) Production of TNF by peritoneal macrophages stimulated for 6 hrs with 10% (v/v) gluten digests by wild-type *E. faecalis* or protease-negative mutants, mean±sem. *p* values

calculated using one-way ANOVA with post-hoc Tukey test, **n** – number of experiments per condition.

(F) IL-6 production by macrophages after overnight stimulation with gluten digests by *E. faecalis* or protease-negative mutants, mean±sem. *p* values calculated using one-way ANOVA with post-hoc Tukey test. **n** – number of experiments per condition.

(G) Comparison of TNF-eliciting activity of gluten digests performed by the wild-type *E. faecalis* strain and by *sprE*$^{-}$ TX5243 or *gelE*$^{-}$ TX5264 mutant strains. Combined results from 5 independent digestions tested independently 2 times. For each batch, TNF levels produced by macrophage incubation with gluten digest by protease-negative JRC105Δ(*gelE*−*sprE*) mutant was subtracted to account for digestion by intracellular proteases from dead bacteria in the culture. mean±sem. *p* values calculated using one-way ANOVA with post-hoc Tukey test.

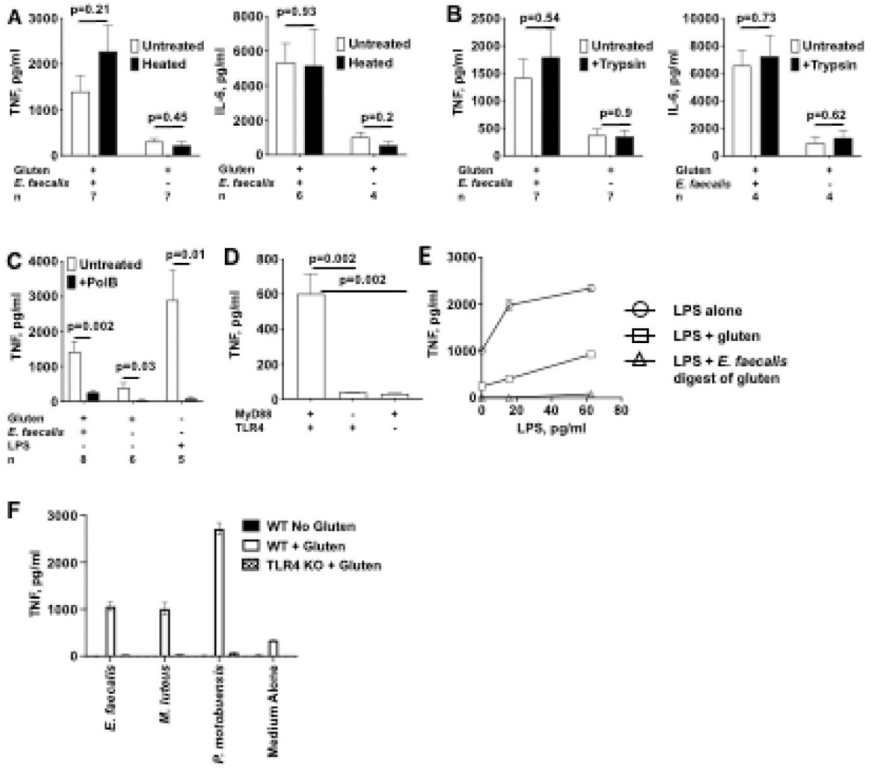

Figure 6. Digestion of gluten by bacterial proteases enhances LPS-triggered production of inflammatory cytokines by macrophages.

(A) Gluten digests in DMEM by *E.faecalis* were heated at 85°C for 30 minutes before adding to macrophages. mean±sem. *p* values calculated using Student's *t* test. **n** – number of experiments per condition.

(B) Same gluten digests were treated with 0.05% Trypsin overnight at 37°C. Mean±sem. *p* values calculated using Student's *t* test, **n** – number of experiments per condition.

(C), Gluten digests were either left untreated or treated with Polymyxin B beads overnight at 4°C. Polymyxin B activity was controlled by simultaneous treatment of LPS (at final concentration of 1 ng/ml). Mean±sem. *p* values calculated using Student's *t* test, **n** – number of experiments per condition.

(D) Stimulation of wild-type NOD and NOD.MyD88 KO or NOD.TLR4 KO macrophages with gluten digested by *E. faecalis*. mean±sem. *p* values calculated using one-way ANOVA with post-hoc Tukey test. Data are from a representative experiment of 4 independent experiments.

(E) Suboptimal dose of LPS (representative experiment of 6 independent experiments, black line) was mixed with undigested gluten (green lines) or *E. faecalis* digest of gluten (red line) and added to macrophages for 6 hours stimulation. Mean±sem.

(F) Bacteria from SI of NOD mouse on HC+4% gluten diet were selected based on either digestion of gliadin or growth on minimal medium with added gluten. TNF secretion by NOD WT or NOD.TLR4 KO macrophages induced with digests by indicated bacteria grown in DMEM with or without gluten. Mean±sem. Representative experiment of three independent experiments.

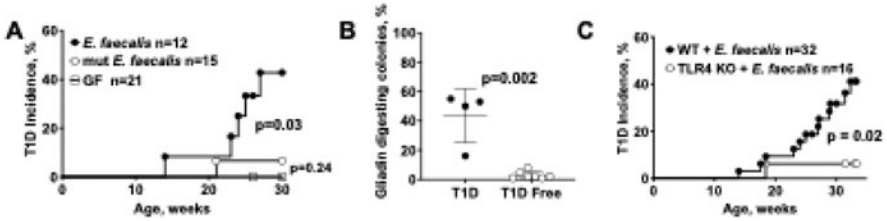

Figure 7. Gluten digestion by secreted microbial proteases is key to T1D promotion.

(A) T1D incidence in GF and gnotobiotic mice colonized with either wild-type *E. faecalis* or mutant bacteria incapable of making secreted proteases and fed with HC+4%gluten diet, *p* values were estimated using Mantel-Cox long-rank test.

(B) Proportion (%) of gliadin-digesting bacteria in the small intestines of ex-GF mice monocolonized with the wild-type *E. faecalis* bacteria at the time of diabetes development or at 30-week endpoint if mice stayed diabetes-free, mean±sem. *p* value was calculated using Student's *t* test. Points represent individual animals.

(C) Comparison of T1D incidence in gnotobiotic wild-type NOD mice of NOD mice lacking TLR4 colonized with *E. faecalis* and fed with HC+4%gluten diet, *p* values were estimated using Mantel-Cox long-rank test.

KEY RESOURCES TABLE

REAGENT or RESOURCE	SOURCE	IDENTIFIER
Antibodies		
Rat Anti-Mouse CD45 (Clone 30-F11), BUV395	BD Biosciences	Cat. 564279; RRID AB_2651134
Rat Anti-Mouse CD4 (Clone GK1.5), BUV496	BD Biosciences	Cat. 741051; RRID AB_2870666
Rat Anti-Mouse CD19 (Clone 1D3), BUV563	BD Biosciences	Cat. 749028; RRID AB_2873425
Rat Anti-Mouse FR4 (Clone 12A5), BUV737	BD Biosciences	Cat. 748995; RRID AB_2873392
Rat Anti-Mouse CD274 (PDL1, Clone MIH5), BV480	BD Biosciences	Cat. 746275; RRID AB_2743606
Rat Anti-Mouse CD62L (Clone MEL-14), BUV805	BD Biosciences	Cat. 741924; RRID AB_2871237
Hamster Anti-Mouse CD80 (Clone 16-10A1), BV711	BD Biosciences	Cat. 740698; RRID AB_2740382
Armenian hamster Anti-Mouse CD11c (Clone N418), BB515	BD Biosciences	Cat. 565586; RRID AB_2869690
Rat Anti-Mouse CD16/CD32 (Fc Block, Clone 2.4G2), Purified	BD Biosciences	Cat. 553142; RRID AB_394656
Rat Anti-Mouse/Human CD44 (Clone IM7), BV510	Biolegend	Cat. 103044; RRID AB_2650923
Armenian hamster Anti-Mouse CD103 (Clone 2E7), BV605	Biolegend	Cat. 121433; RRID AB_2629724
Hamster Anti-Mouse CD279 (PD-1, Clone J43), BV650	BD Biosciences	Cat. 744546; RRID AB_2742317
Armenian hamster Anti-Mouse CD69 (Clone H1.2F3), BV785	Biolegend	Cat. 104543; RRID AB_2629640
Rat Anti-Mouse/Human CD11b (Clone M1/70), PerCP-Cy5.5	Biolegend	Cat. 101227; RRID AB_893233
Rat Anti-Mouse F4/80 (Clone BM8), PE-Dazzle 594	Biolegend	Cat. 123145; RRID AB_2564132
Rat Anti-Mouse CD86 (Clone PO3), PE-Cy7	Biolegend	Cat. 105115; RRID AB_493601
Armenian hamster Anti-Mouse TCR β chain (Clone H57-597), Alexa Fluor 700	Biolegend	Cat. 109223; RRID AB_1027654
Rat Anti-Mouse CD8a (Clone 53-6.7), APC-Fire 750	Biolegend	Cat. 100765; RRID AB_2572112
Armenian hamster Anti-Mouse CD152 (CTLA-4, Clone UC10-4B9), PE	Biolegend	Cat. 106305; RRID AB_313254
Rat Anti-Mouse Ki67 (Clone 16A8), Alexa Fluor 647	Biolegend	Cat. 652407; RRID AB_2562138
Armenian hamster Anti-Mouse CD11c (Clone N418), APC	Biolegend	Cat. 117309; RRID AB_313778
Rat Anti-Mouse/Human CD11b (Clone M1/70), FITC	Biolegend	Cat. 101205; RRID AB_312788
Rat Anti-Mouse TNFa (Clone MP6-XT22), BV421	Biolegend	Cat. 506327; RRID AB_10900823
Armenian Hamster Anti-Mouse CD3ε (Clone 145-2C11), PE	Biolegend	Cat. 100307; RRID AB_312672
Rat Anti-Mouse FoxP3 (Clone FJK-16S), efluor-450	Thermo/Fisher	Cat. 48-5773-82; RRID AB_1518812
Rat Anti-Mouse/Human/Bovine Insulin (Clone 182410), APC	R&D Systems	Cat. IC1417A; RRID AB_2126535
Sheep anti-Mouse/Rat Transglutaminase 2/TGM2 Antibody	R&D Systems	Cat. AF5418; RRID AB_2044738
Donkey anti-Sheep IgG HRP-conjugated Antibody	R&D Systems	Cat. HAF016; RRID AB_562591
Anti-β-Actin Antibody (Clone C4)	Santa Cruz Biotechnology	Cat. sc-47778; RRID AB_626632
Amersham Sheep Anti-Mouse Horse Radish Peroxidase Antibody	GE Healthcare	Cat. NA93; RRID AB_772210
Armenian Hamster Anti-Mouse CD3e (Clone 145-2C11), PE	Thermo/Fisher	Cat. 12-0031-82; RRID AB_465496
Rat Anti-Mouse CD4 (Clone GK1.5), APC	Biolegend	Cat. 100412; RRID AB_312697
Armenian Hamster Anti-Mouse TCR β chain (Clone H57-597), FITC	Biolegend	Cat. 109205; RRID AB_313428
Rat Anti-Mouse CD8a (Clone 53-6.7) efluor450	Thermo/Fisher	Cat. 48-0081-82; RRID AB_1272198
Rat Anti-Mouse TotalSeq™-C0302 (Clone M1/42; 30-F11)	Biolegend	Cat. 155863; RRID AB_2800694

REAGENT or RESOURCE	SOURCE	IDENTIFIER
Rat Anti-Mouse TotalSeq™-C0303 (Clone M1/42; 30-F11)	Biolegend	Cat. 155865; RRID AB_2800695
Rat Anti-Mouse TotalSeq™-C0305 (Clone M1/42; 30-F11)	Biolegend	Cat. 155869; RRID AB_2800697
Rat Anti-Mouse TotalSeq™-C0306 (Clone M1/42; 30-F11)	Biolegend	Cat. 155871; RRID AB_2819910
Rat Anti-Mouse TotalSeq™-C0308 (Clone M1/42; 30-F11)	Biolegend	Cat. 155875; RRID AB_2819912
Rat Anti-Mouse TotalSeq™-C0309 (Clone M1/42; 30-F11)	Biolegend	Cat. 155877; RRID AB_2819913
Bacterial and Virus Strains		
Enterococcus faecalis Str. OG1RF	Murray et al. 1993.	NCBI:txid474186
Enterococcus faecalis Str. TX5266	Qin et al. 2001.	N/A
Enterococcus faecalis Str. TX5243	Sifri et al. 2002.	N/A
Enterococcus faecalis Str. TX5264	Singh et al. 1998.	N/A
Enterococcus faecalis Str. JRC105	Kristich et al. 2007.	N/A
Chemicals, Peptides, and Recombinant Proteins		
Dextrose (D-Glucose) Anhydrous	Fisher Scientific	Cat. D16-500
Insulin Solution Human	Sigma-Aldrich	SKU: I9278-5ML,
Erythromycin	Sigma-Aldrich	SKU: E5389-1G
Nicin from Lactococcus lactis 2.5% (balance sodium chloride)	Sigma-Aldrich	SKU: N5764-1G
BBL Brain Heart Infusion Agar	BD Difco	Item no. 211065
Bacto Brain Heart Infusion	BD Difco	Item no. 237500
5(6)-CFDA, SE; CFSE (5-(and-6)-Carboxyfluorescein Diacetate, Succinimidyl Ester), mixed isomers	Invitrogen	Cat. C1157
Polymyxin B-Agarose	Sigma-Aldrich	SKU: P1411-5ML
DMEM, high glucose, GlutaMAX supplement	Gibco	Cat. 10566-016
Cell Dissociation Buffer Enzyme-Free PBS-Based	Gibco	Cat. 13151-014
0.5% Trypsin-EDTA 10X	Gibco	Cat. 15400-054
Click's Medium	Irvine Scientific	Cat. 9582
Histopaque-1119	Sigma-Aldrich	Cat. 11191
SuperSignal™ West Femto Maximum Sensitivity Substrate	Thermo Scientific	Cat. 34095
Pierce Protease Inhibitor Tablets	Thermo Scientific	Cat. A32963
Thioglycollate Medium without Dextrose	BD Difco	Cat. DF0363-17-2
Collagenase P from *Clostridium histolyticum*	Roche	SKU: 11213857001
Collagenase D from *Clostridium histolyticum*	Roche	SKU: 11088858001
Deoxyribonuclease I from bovine pancreas	Sigma-Aldrich	SKU: DN25-10MG
Whetpro 80 Gluten	ADM	https://www.adm.com/products-services/food/adm-milling/products/wheat-glutens/wheat-gluten
Protein Transport Inhibitor (Containing Brefeldin A)	BD Biosciences	Cat. 555029; RRID AB_2869014
Gliadin from Wheat	Sigma Aldrich	SKU: G3375
Casein, Bovine Milk	Sigma Aldrich	SKU: 281680
Bovine Serum Albumin (BSA) (Fraction V) Heat-Shock Treated	Fisher Scientific	Cat. BP1600-100
NRPA7 Peptide (KYNKANAFL)	Sigma Aldrich	N/A

REAGENT or RESOURCE	SOURCE	IDENTIFIER
AI4 Mimotope Peptide (YFIENYLEL)	Sigma Aldrich	N/A
InsB15-23 Peptide (LYLVCGERG)	Sigma Aldrich	N/A
DQ8-glia-alpha1 Peptide (SGEGSFQPSQENPQ)	Sigma Aldrich	N/A
DQ2.5-glia-omega2 Peptide (FPQPEQPFPWQP)	Sigma Aldrich	N/A
Critical Commercial Assays		
Diastix Reagent Strips for Urinalysis, Glucose	Ascensia Diabetes Care, Purchased from Walmart	Model: 00193-2802-50
OneTouch UltraMini Blood Glucose Meter	OneTouch Solutions	N/A
GenUltimate! Test Strips	GenUltimate!	UPC: 868906000100
CD4+ T Cell Isolation Kit	Miltenyi Biotec	Cat. 130-104-454
Mouse TNF ELISA Set II	BD Biosciences	Cat. 558534; RRID AB_2869215
ELISA MAX™ Standard Set Mouse IL-6	Biolegend	Cat. 431301
ELISA MAX™ Standard Set Mouse IL-2	Biolegend	Cat. 431001
eBioscience™ Foxp3 / Transcription Factor Staining Buffer Set	Invitrogen	Cat. 00-5523-00
Zombie NIR™ Fixable Viability Kit	Biolegend	Cat. 423105
Chromium Single Cell 3’ Library & Gel Bead Kit	10X Genomics	PN-120237
Chromium Single Cell Mouse TCR Amplification Kit	10X Genomics	PN-1000254
Chromium Single Cell 5’ Library Construction Kit	10X Genomics	PN-1000020
Chromium Single Cell 5’ Library & Gel Bead Kit	10X Genomics	PN-1000014
UltraComp eBeads™ Compensation Beads	Invitrogen	Cat. 01-2222-41
DNeasy PowerSoil HTP 96 Kit	Qiagen	Cat. 12955-4
UltraClean 96 PCR Cleanup Kit	Qiagen	Cat. 12596-4
Quant-iT™ PicoGreen™ dsDNA Assay Kits and dsDNA Reagents	Invitrogen	Cat. P7589
Limulus Amoebocyte Lysate (LAL) kinetic chromogenic test kit Endochrome-K	Charles River	Code R1708K
Endotoxin Specific Buffer for LAL Assay	Charles River	Code BG120
Endotoxin free 96 well plates for LAL assay	Greiner Bio-One GmbH	Cat. 655101
Mouse IFN-γ ELISPOT Pair	BD Biosciences	Cat. 551881
HRP Streptavidin for ELISPOT	BD Biosciences	Cat. 557630
MultiScreen-IP Filter Plate, 0.45 μm, white, sterile	Millipore-Sigma	Cat. S2EM004M99
Mouse Insulin ELISA Kit	Alpco	Ref. 80-INSMS-E01
Deposited Data		
Raw and analyzed scRNA-Seq on NOD.SCID islets	This paper.	GEO: GSE217495
Raw and analyzed scRNA-Seq on NOD/ShiLtJ islets	This paper.	GEO: GSE217493
Raw and analyzed scTCR-Seq on NOD/ShiLtJ islets	This paper.	GEO: GSE218336
16S rRNA Sequencing	This paper.	https://github.com/akds/microbiome-T1D
Experimental Models: Cell Lines		
578_BV7_AV12: BW58α-β cells expressing human CD4 and TCR from a DQ2.5-glia-ω2–reactive CD4 T cell clone (TCC 578)	Dahal-Koirala et al. 2016.	N/A

REAGENT or RESOURCE	SOURCE	IDENTIFIER
Human Lymphoblastoid Cell Line Expressing HLA-DQ2.5	Generous Gift from Dr. Carole Ober, The University of Chicago	N/A
TCC489.2.1.4 hybridoma recognizing DQ8-glia-alpha1	Qiao et al. 2011.	N/A
Experimental Models: Organisms/Strains		
Mouse: NOD.TLR4 KO	Burrows et al. 2015. Bred in house.	N/A
Mouse: NOD.TGM2 KO	This paper	N/A
Mouse: NOD.Cg-Tg(TcraBDC2.5,TcrbBDC2.5)1Doi/DoiJ; (NOD.BDC2.5)	The Jackson Laboratory	Stock No: 004460; RRID:IMSR_JAX:004460
Mouse: NOD.Cg-*Prkdc*^{scid}/J; (NOD.SCID)	The Jackson Laboratory	Stock No: 001303; RRID:IMSR_JAX:001303
Mouse: NOD.129P2(C)-*Tcra*^{tm1Mjo}/DoiJ; (NOD.TCRa KO)	The Jackson Laboratory	Stock No: 004444; RRID:IMSR_JAX:004444
Mouse: NOD/ShiLtJ	The Jackson Laboratory	Stock No: 001976; RRID:IMSR_JAX:001976
Mouse: NOD.MyD88 KO	Wen et al. 2008. Bred in house	N/A
Oligonucleotides		
Genotyping and 16S Amplicon Primers (Table S1)	This paper	N/A
Tgm2 Guide RNA: >sgRNA 1745 - EXON 1 GTCGCCGCTAGCGTGG/CCA	This paper	N/A
Tgm2 Guide RNA: >sgRNA 1747 - EXON 2 GATTTGGAGATTCAGGC/CAA	This paper	N/A
Recombinant DNA		
pMSP3535: Shuttle vector with Nisin Inducible Promoter	Bryan et al. 2000.	NCBI:txid244879; RRID:Addgene_46886
pMSP3614: pMSP3535 containing *gelE* following the Nisin inducible promoter.	Waters et al. 2003.	N/A
Software and Algorithms		
BD FACSDiva v. 8.0.2	BD Biosciences	https://www.bdbiosciences.com/en-us/products/software/instrument-software/bd-facsdiva-software
SpectroFlo v. 2.2.04	Cytek Biosciences	https://cytekbio.com/pages/spectro-flo
FlowJo v. 10.7.1	FlowJo	https://www.flowjo.com/solutions/flowjo/downloads
UMAP Plugin v. 3.1	McInnes et al. 2020.	https://www.flowjo.com/exchange/#/plugin/profile?id=6
R v. 3.6.3	The R Project for Statistical Computing	https://cran.r-project.org/bin/macosx/
Python v. 3.7.4	Python Software Foundation	https://www.python.org/downloads/macos/
MATLAB v. R2020a	MathWorks	https://www.mathworks.com/products/matlab/whatsnew.html
CellRanger v.4.0.0	10X Genomics	https://support.10xgenomics.com/single-cell-gene-expression/software/downloads/latest?
Seurat v. 3.1.5	Hao et al. 2021.	https://satijalab.org/seurat/articles/install.html
Scanpy v. 1.4.5.1	Wolf et al. 2018.	https://pypi.org/project/scanpy/

REAGENT or RESOURCE	SOURCE	IDENTIFIER
Scirpy v. 0.10.1	Sturm et al. 2020.	https://github.com/scverse/scirpy
Seaborn v. 0.11.2	Waksom. 2021.	https://seaborn.pydata.org/
GSEA v. 4.1.0	Mootha et al. 2003 and Subramanian et al. 2005.	http://www.gsea-msigdb.org/gsea/downloads.jsp
STRING v. 11.0	Szklarczyk et al. 2011.	https://string-db.org/cgi/input?sessionId=bfTlTaC7SUO2&input_page_show_search=off
QIIME v. 1.9	Caporaso et al. 2010.	http://qiime.org/index.html
Prism v. 9.1.2	GraphPad	https://www.graphpad.com/
Other		
16% Hydrolyzed Casein + 4% WhetPro 80 Gluten Custom Diet	Envigo	TD.150366
16% Hydrolyzed Casein + 4% Gem of the West Gluten Custom	Envigo	TD.130340
NIH-31 Modified Open Formula Mouse/Rat sterilizable diet	Envigo	7013
20% Hydrolyzed Casein Custom Diet	Envigo	TD.120338
20% Intact Casein Custom Diet	Envigo	TD.120337